4-22-2016

Upper Albian to Lower Cenomanian Calcareous Nannofossil Biostratigraphy of the Proto-North Atlantic

Shamar Chin
University of Nebraska-Lincoln, shamar.chin@huskers.unl.edu

UPPER ALBIAN TO LOWER CENOMANIAN CALCAREOUS NANNOFOSSIL BIOSTRATIGRAPHY OF THE PROTO-NORTH ATLANTIC

by

Shamar Crystal - Ann Chin

A THESIS

Presented to the Faculty of

The Graduate College at the University of Nebraska

In Partial Fulfillment of Requirements

For the Degree of Master of Science

Major: Earth and Atmospheric Sciences

Under the Supervision of Professor David K. Watkins

Lincoln, Nebraska

May, 2016

UPPER ALBIAN TO LOWER CENOMANIAN CALCAREOUS NANNOFOSSIL BIOSTRATIGRAPHY OF THE PROTO-NORTH ATLANTIC

Shamar Crystal - Ann Chin, M.S.

University of Nebraska, 2016

Advisor: David K. Watkins

Lower Cenomanian calcareous nannofossil assemblages from Deep Sea Drilling Project (DSDP) Sites 137 and 547 in the proto-North Atlantic Ocean were analyzed quantitatively to examine the fidelity of the widely used CC and UC calcareous nannofossil Zonal schemes. Datasets from Ocean Drilling Program (ODP) holes 1050C and 1052E (Blake Nose) and Tanzania Drilling Project (TDP) Site 24 were integrated into this dataset.

Four biozones spanning the upper Albian through middle Cenomanian were determined using the method of unitary associations (UA). Data were also used from these sequences to generate a ranking and scaling (RASC) optimum sequence. A new reliability index method that uses binomial probabilities is proposed because the existing method does not work well for Mesozoic taxa due to patchy distribution and lower abundances. Three bioevents, *Gartnerago stenostaurion* - LAD, *Lithraphidites eccentricum* - FAD, and *Staurolithites mutterlosei* - LAD, were shown to be reliable markers for lower Cenomanian biostratigraphy based on the new reliability index values. This study also corroborates the lower Cenomanian FAD of *Lithraphidites eccentricum*, whereas the FAD of *Cylindralithus scultpus* and the LAD *Zeugrhabdotus xenotus* appear to be more effective as regional rather than global markers, due to discrepancies in

superpositional relationships in these sections. A biostratigraphic framework improved the age model for DSDP Leg 79, Site 547 by documenting an expanded section across the Albian/Cenomanian boundary at Site 547 based on the LAD of *Corollithion kennedyi*. A revised age model for DSDP Leg 14, Site 137 now includes an older age into the upper Albian - middle Cenomanian. Site 547 had a higher diversity of holococcoliths than Site 137. *Calculites anfractus,* an important marker species, was proposed as a nannofossil marker species associated with the Global boundary Stratotype Section and Point (GSSP) for the base of the Cenomanian; however, it does not occur globally. Controls on holococcolith distribution are poorly understood and are likely controlled by oceanic setting. *C. anfractus* may be controlled by these factors, and as such, is not a reliable nannofossil marker for the Albian/Cenomanian boundary.

Acknowledgements

Samples for this study were obtained from the Deep Sea Drilling Project (DSDP) and the Ocean Drilling Program (ODP). DSDP and ODP are sponsored by the National Science Foundation (NSF) and participating countries under the management of Joint Oceanographic Institutions (JOI), Inc. The Tanzania Drilling Project (TDP), from which samples were obtained, is supported primarily by the United Kingdom's Natural Environment Research Council (NERC), but collaborators from the United Kingdom, Tanzania, Ireland, the Netherlands, and the United States have contributed. I would like to thank my committee members, Tracy Frank and David Harwood, for providing me with great feedback and improving this manuscript, and my advisor, David Watkins, for guiding me through this process and making this project possible.

TABLE OF CONTENTS **PAGE**

LIST OF FIGURES **PAGE**

LIST OF TABLES **PAGE**

1. Introduction

The mid-Cretaceous marks a time of fundamental change in Earth's history, including extreme greenhouse conditions, rapid sea-floor spreading rates, and the onset of widespread chalk deposition (Haq et al., 1987; Clarke and Jenkyns, 1999; Huber et al., 2002; Wilson et al., 2002; Moriya et al., 2007; Friedrich et al., 2008; Hay, 2008; Brace and Watkins, 2015). In order to address global paleoceanographic questions about these events, it is critical to be able to correlate stratigraphic sections across ocean basins. The Albian/Cenomanian boundary marks a transitional point during the mid-Cretaceous; however, the Albian and Cenomanian stages occurred during the Cretaceous polarity Normal Superchron (C34). Because this is a particularly long chron, magnetic reversals cannot be used for age control, making biostratigraphy an integral tool in correlation of marine strata of this age. The mid-Cretaceous is also characterized by Oceanic Anoxic Events (OAEs) where stratigraphic records of bulk carbonate isotopes show positive carbon isotope excursions that are correlatable across wide geographic regions (Jenkyns et al., 1994; Erbacher et al., 1996). Without these isotope excursions, it is difficult to correlate intervening periods, which further increases the value of biostratigraphy during this time.

While biostratigraphic zonation schemes exist for the Cretaceous, the CC Zonations (Perch-Nielsen, 1985) and UC Zonation (Burnett et al. 1998) uses marker species from the Tethyan realm. During the mid-Cretaceous, the Atlantic Ocean was narrow and divided latitudinally by the Equatorial Atlantic Gateway (EAG), which started opening at approximately 120 Ma (Hay et al., 1999; Pletsch et al., 2001; Jacobs et al., 2009). The proto-North Atlantic was a mid-latitude ocean that connected to the

Tethys Ocean, but a widely used biostratigraphic framework does not exist for this region. Specific goals of this study include testing the reliability of the Perch-Nielsen (1985) and Burnett et al. (1998) marker species in the proto-North Atlantic using a new Reliability Index method that is proposed in the current study. This entails correlating the observed bioevents across all sites, which will allow development of a biostratigraphic scheme using co-occurrences of these species, as well as an optimum sequence of bioevents. The resulting biostratigraphic framework is compared to the widely used CC Zonation (Perch-Nielsen, 1985) and the UC Zonation (Burnett et al., 1998). These zonation schemes are illustrated in Fig. 2. This study analyzes quantitatively lower Cenomanian samples from proto-North Atlantic sites from DSDP Leg 14, Site 137 and DSDP Leg 79, Site 547 (Fig.1) by obtaining absolute abundance data and applying probabilistic and deterministic biostratigraphic methods to this data. In addition to analyzing these samples quantitatively, ODP Leg 171B, sites 1050 and 1052 (Watkins, unpublished) and the Tanzania Drilling Project (TDP), Site 24 (Ando et al., 2015) datasets are integrated with datasets from this study and analyzed statistically.

A taxon of particular interest is *Calculites anfractus* because the FAD of *Calculites anfractus* was designated as a secondary calcareous nannofossil marker for the basal Cenomanian (Kennedy et al., 2004). However, *Calculites anfractus* is rarely reported in the literature and it is necessary to test its utility a global marker.

Identifying discrepancies in the data will ultimately allow for greater accuracy and increased resolution of biostratigraphic schemes when correlating these bioevents. This study aims to identify and where possible, assess these discrepancies and refine the current biostratigraphic frameworks.

2. Materials

A total of six localities were considered for this study, but only sites 137 and 547 had high nannofossil abundances and good preservation making them ideal for a quantitative study.

DSDP Leg 14, Site 137

DSDP Leg 14, Site 137 is located in the North Atlantic Ocean at 25° 55.53' N, 27° 03.64' W, approximately 1000 kilometers west of Cap Blanc, Mauritania, close to the base of the continental rise at a water depth of 5361 meters. Thirty-two samples from Cores 8 through 16 (267.76 to 380.82 mbsf) were examined based on Bukry's (1972) original age assignment of Albian and Cenomanian. These cores consist of banded and partly laminated greenish to brownish nannoplankton marl to chalk, with intermittent, carbonate-poor silty layers. The nannofossil assemblages exhibit good to poor preservation.

DSDP Leg 79, Site 547

DSDP Leg 79, Site 547 is located in the North Atlantic Ocean at 33° 46.84' N, 09° 20.98' W, on the West African margin west of Morocco at a water depth of 3940.5 meters (Fig. 1). This site is located on the northeastern flank of a northwest-trending ridge in front of the Mazagan Plateau. Forty-one samples from Cores 40 through 64 (431.18 to 659.28 mbsf) were examined based on the original age assignment of Albian - upper Cenomanian (Wiegand, 1984). The lithology is predominantly greenish to grayish nannofossil chalk and nannofossil-bearing claystone with layers of flat-pebble claystone conglomerate. The upper Albian through upper Cenomanian succession is approximately 350 meters thick, with an average sediment accumulation rate of 29 m/m.y. (Leg 79

Shipboard Scientific Party, 1984). This sequence is overlain by Campanian clayey nannofossil and foraminiferal-nannofossil chalk and separated by a disconformity with a hiatus of 14 to 19 m.y. (Leckie, 1984).

Acquired Datasets

In order to gain more complete coverage of the proto-North Atlantic Ocean biostratigraphy, datasets from ODP Leg 171B, sites 1050 and 1052 from Blake Nose were obtained from Watkins (unpublished). Blake Nose is located in the Atlantic Ocean, east of Florida at 30°5.9953′ N, 76°14.0997′ W at a water depth of 2296.5 meters (Holes 1050C and 1052E. An additional dataset, Tanzania Drilling Project (TDP) Site 24 from the Indian Ocean, was acquired in order to compare the proto-North Atlantic biostratigraphy to that of the Proto-Indian Ocean. TDP Site 24 has a lower Cenomanian section with exceptionally well-preserved nannofossils and planktonic foraminifera, and refined age-control (Ando et al., 2015).

3. Methods

Smear slides of 73 samples were analyzed: 32 samples from DSDP Site 137 and 41 samples from DSDP Site 547. Samples were prepared using the double-slurry method (Watkins and Bergen, 2003). Species abundances were determined by counting approximately 500 specimens. Two additional traverses were scanned for rare species. Counts were obtained using an Olympus BX51 light microscope at a total magnification of 1250x, using cross-polarized and plane-polarized light, and a one-quarter λ gypsum plate.

State of preservation was determined using the scheme of Watkins and Bowdler (1984). The criteria are as follows:

- Good - A vast majority of the specimens could be identified to the species level;
- Moderate - A significant portion of the specimens were hard to identify due to overgrowth and/or dissolution;
- Poor – A majority of the specimens could not be identified to the species level due to severe dissolution, fragmentation and/or overgrowth.

Estimating nannofossil abundance as a sedimentary component follows Watkins and Bowdler (1984). All abundances were estimated from smear slides of raw sediment using the following criteria:

- Abundant - nannofossils comprise more than 15% of the sediment
- Common - nannofossils comprise 5-15% of the sediment
- Few - nannofossils comprise 1-5% of the sediment
- Rare - nannofossils comprise less than 1% of the sediment
- Essentially barren - nannofossils significantly less than 1% of the sediment, typically fewer than 10 specimen per 100 fields-of-view
- Barren - no nannofossils observed in 100 fields-of-view

For the purposes of counting, some nannofossils were grouped together at the genus level and assigned "spp." to indicate the presence of multiple species. After scanning and attempting to analyze quantitatively each sample at the species level, genera such as *Calculites*, *Helicolithus*, *Manivitella*, *Retecapsa*, *Staurolithites*, *Tranolithus*, and *Zeugrhabdotus* were noted to have many morphotypes; however, many of the species have no biostratigraphic significance. Examples include *Tranolithus bitraversus*, *Tranolithus exiguus*, *Tranolithus gabalus*, and *Tranolithus orionatus*. In addition to thegenera mentioned above, unidentifiable holococcoliths were grouped together as well.

Unitary Associations (UA) and Ranking and Scaling (RASC)

The CC (Perch-Nielsen, 1985) and UC (Burnett et al., 1998) zonations are qualitative schemes based on concurrent and partial range zones. Intervals are defined by documenting the lowest occurrence of one or more diagnostic taxa and the highest occurrence of other taxa. In order to test the validity of these zonation schemes, two quantitative methods, unitary associations (UA) and ranking and scaling (RASC), were chosen for data analysis.

Unitary associations (UA) is a deterministic mathematical method for constructing a set of mutually exclusive concurrent range zones. Two species are defined as compatible if their chronologic co-occurrence has been observed (= real association) or can be deduced from biostratigraphic data (= virtual association), where a UA is a maximal set of compatible species (Guex, 1991).

Ranking and scaling (RASC) is a probabilistic method that produces the order of biostratigraphic events that occur based on observations from multiple localities. Such events can be the first and/or last appearance datums (FAD and/or LAD) of a certain taxa, or an abundance peak (bloom). Ranking is the first step of this method, which involves ordering the events. This order is achieved by a 'majority vote', counting the number of times each event occurs above, below or together with all others. Scaling is the second step of this method, for which distances between consecutive events are estimated and stratigraphic positions at multiple localities can be determined (Gradstein et al., 1985; Agterberg, 1990; Agterberg & Gradstein, 1999). A total of 179 samples and 275 taxa are included in the raw database. The PAleontological STatistics (PAST) program was used to perform the UA and RASC analyses.

Reliability Indices

Biostratigraphic accuracy of data were analyzed using Reliability Index methods proposed by Bralower et al. (1988) and Bergen et al. (2013) for sites 137 and 547. The additional three datasets were not used in this analysis due to the requirement of absolute counts abundance data, which are not available for ODP Holes 1050C and 1052E. While fully quantitative abundance data are available for TDP Site 24, many of the markers discussed are absent at this site, so it is excluded. Marker species were selected from the CC (Perch-Nielsen, 1985) and UC (Burnett et al., 1998) zonation schemes, as well as species identified from the UA and RASC analyses.

The method proposed by Bralower et al. (1988) includes a quantitative index that uses average stratigraphic sample spacing and the distribution and abundance of species above and below the level of its first or last occurrence, respectively. The Bralower et al. (1988) Reliability Index, R, is calculated using the following equation:

$$R = Z \sum_{i=1}^{n} x_i ((n+1)-i)/100$$

where

- Z = Average number of samples per unit thickness
- n = Number of values over which Reliability Index is calculated
- x_i = Number of specimens of marker species in the *i*-th sample
- (n+1)-*i* = Used to scale index linearly
- 100 = Arbitrarily chosen divisor to reduce range of indices

Ten was chosen for the n-value, as this is the optimal range for nearing the end of a species stratigraphic range (Bralower et al., 1988; Bergen at al., 2013).

Bergen et al. (2013) proposed two methods for calculating Reliability Index, both are modified versions of Bralower et al. (1988).

1. The number of samples in which a species was observed in either the top or bottom ten samples of its stratigraphic range.

2. The percentage of samples a species was found throughout its entire documented stratigraphic range.

Bralower et al. (1988) have shown that the distribution of marker species in the Mesozoic is patchy and abundances are lower compared to the Cenozoic, ultimately reflecting much lower reliability index values. A goal of this project is to test the reliability of marker species, and evaluate the impact of patchy distribution in reducing their reliability.

An alternative method is presented here that uses binomial probabilities to determine the probability of success of finding a given marker over its stratigraphic range. This is modeled after the Bernoulli trials (or Binomial trial), where independent events are described as "successes" or "failures". The first step in this process is to establish the number of successes and failures for each species for a given stratigraphic interval.

$$\binom{n}{x} p^x (1-p)^{n-x}$$

where

- n = Number of fixed trials; 10 was chosen for this study
- x = Specified number of successes
- p = Probability of success through a stratigraphic interval

The specified number of successes has been chosen to be 0.95; therefore, the probability of failure is 0.05. The following equation was used to determine the probability distribution for any given species over the chosen stratigraphic range:

$$\binom{n}{x} = \frac{n!}{x!(n-x)!}$$

Deriving the Log Base 10 for each value followed the above step; the absolute value for each result was used. This was done in order to make the initial values larger and limit them to a smaller range, ultimately making the results easier to manage.

4. Results

Albian - Cenomanian Biochronology

Samples are classified biostratigraphically using modified versions (Fig. 2) of the CC Zonation of Perch-Nielsen (1985) and the UC Zonation of Burnett at al. (1998). In this study, a total of 193 taxa were identified and 16 bioevents were selected on the basis of the FAD and LAD for comparison to these zonation schemes. Table 1 lists bioevents for DSDP Site 137 (this study), DSDP Site 547 (this study), ODP Holes 1050C & 1052E (Watkins, unpublished) and TDP Site 24 (Ando et al., 2015). Fig.3 shows the position of bioevents for Site 137, and Fig. 4 shows the position of bioevents for Site 547.

Albian - Cenomanian Biochronology for DSDP Leg 14, Site 137

Samples 137-16R-3, 135-136 cm and 137-16R- 4, 131-132 cm (379.36 and 380.82 mbsf, respectively) contain abundant, moderate to well-preserved nannofossil assemblages that include *Axopodorhabdus biramiculatus*, *Gartnerago stenostaurion*, *Eiffellithus paragogus*, *Eiffellithus turrisseiffelii*, and *Hayesites albiensis*. *Corollithion kennedyi* was not present in these two samples. This assemblage is diagnostic of uppermost Albian Subzone CC9a (= BC27/UC0a).

Samples 137-15R-1, 111-112 cm through 137-16R-2, 140-141 cm (349.12-377.91 mbsf) contain abundant, poor to well-preserved nannofossil assemblages that include

Axopodorhabdus biramiculatus, *Gartnerago stenostaurion*, *Eiffellithus paragogus*, *Eiffellithus turrisseiffelii*. *Corollithion kennedyi* and *Hayesites albiensis* were not present in these samples. This assemblage is diagnostic of the uppermost Albian through the Albian - Cenomanian (A/C) boundary Subzone CC9b (=BC27/UC0b).

Sample 137-14R-6, 120-121 cm (347.71 mbsf) contains abundant, well-preserved nannofossil assemblages that include *Axopodorhabdus biramiculatus*, *Gartnerago stenostaurion*, *Eiffellithus paragogus*, *Eiffellithus turrisseiffelii*, and *Corollithion kennedyi*. The FAD of *C. kennedyi* occurs at 100.45 Ma; this is 0.05 Ma after the Albian/Cenomanian boundary (Gradstein et al., 2012). This assemblage is diagnostic of the lowermost Cenomanian Subzone CC9b (=UC1a). It is important to note that sample 137-14R-6, 120-121 cm (347.71 mbsf) is a part of a condensed section where numerous co-occurring bioevents were observed. The FAD of *Corollithion kennedyi*, LAD of *Gartnerago stenostaurion, LAD* of *Gartnerago chiasta*, FAD of *Discorhabdus watkinsii,* FAD of *Lithraphidites eccentricum*, and LAD of *Watznaueria britannica* are all observed in this sample.

Samples 137Z-10R-2, 104-105 cm through 137Z-14R-6, 120-121 cm (285.55-347.71 mbsf) contain abundant, moderate to well-preserved nannofossil assemblages that include *Corollithion kennedyi*, *Helenea chiastia*, and *Axopodorhabdus biramiculatus* occur through the section, while *Lithraphidites acutus*, the nannofossil marker for the basal middle Cenomanian (Gradstein et al., 2012) was not present in these samples. This assemblage is diagnostic of lower Cenomanian Subzone CC9b (=UC1/2).

Samples 137Z-8R-2, 125-126 cm through 137Z-10R-1, 102-103 cm (267.76-284.03 mbsf), contain abundant, poor to well-preserved nannofossil assemblages that include

Corollithion kennedyi, *Helenea chiastia*, *Axopodorhabdus biramiculatus,* and *Lithraphidites acutus.* This assemblage is diagnostic of the middle Cenomanian Subzone CC10a (=UC3a).

Albian - Cenomanian Biochronology for DSDP Leg 79, Site 547

Sample 547A-64-1, 27.5-29 cm (659.28 mbsf) contains abundant, moderately-preserved nannofossil assemblages that include *Axopodorhabdus biramiculatus, Gartnerago stenostaurion, Eiffellithus paragogus*, *Eiffellithus turrisseiffelii*, and *Hayesites albiensis*. *Calculites anfractus* and *Corollithion kennedyi*, were not present in this sample. This assemblage is diagnostic of the uppermost Albian Subzone CC9a (=BC27/UC0a)

Sample 547A-63-1, 26.5 -28 cm and (649.78 mbsf) contains abundant, well-preserved nannofossil assemblages that include *Axopodorhabdus biramiculatus*, *Gartnerago stenostaurion, Eiffellithus paragogus*, and *Eiffellithus turrisseiffelii*. *Calculites anfractus*, *Corollithion kennedyi,* and *Hayesites albiensis* were not present in this sample. This assemblage is also diagnostic of the uppermost Albian Subzone CC9a (=BC27/UC0a).

Samples 547A-59-6, 8-9 cm through 547A-62-3, 50-51 cm (619.9-643.51 mbsf) contain abundant, moderate to well-preserved nannofossil assemblages that include *Axopodorhabdus biramiculatus, Gartnerago stenostaurion, Eiffellithus paragogus, Eiffellithus turrisseiffelii*, and *Calculites anfractus*. *Corollithion kennedyi* and *Hayesites albiensis* were not present in these samples. This assemblage is diagnostic of strata associated with the Albian/Cenomanian boundary. The FAD of *Corolllithion kennedyi* is observed in sample 547A-51-4, 112-113 (542.13 mbsf) and is

used to mark the upper limit of this zone. Therefore, the FAD of *C. anfractus* and *C. kennedyi* (632.51 and 542.13 mbsf, respectively) indicate the presence of strata associated with the boundary.

Samples 547A-40-1, 18 cm through 547A-50-4, 22-23 cm contain abundant, poor to well-preserved nannofossil assemblages that include *Corollithion kennedyi*, *Helenea chiastia*, and *Axopodorhabdus biramiculatus. Lithraphidites acutus* was not present in these samples. This assemblage is diagnostic of lower Cenomanian Subzone CC9b (=UC1/2).

Correlation of Bioevents: Cross Plots

In order to visualize the sequence of events for the sites in this study, a cross plot was created to show the position of bioevents relative to each other. Three additional acquired datasets (DSDP holes 1050C, 1050E, and TDP Site 24) were also used for correlation. Bioevents that are calibrated to the geologic time scale, UC and CC Zonation marker species and bioevents observed in this study were used to generate the cross plots (Fig. 5).

The crossing of lines indicates differences in the relative order of bioevents from section to section. Table 2 shows 10 of the 16 identified species with their assigned ages from the geologic time scale (Gradstein et al., 2012). The numbers 1- 10 indicate the chronological order in which these events should occur, with 1 being the oldest bioevent and 10 being the youngest bioevent. This is based on assignments from the 2012 geologic time scale (Gradstein et al., 2012) in conjunction with the type level age assignments. The events highlighted in grey do not occur in chronological order in these sections.

The LAD of *Gartnerago stenostaurion* was assigned to the uppermost Albian (Burnett at al., 1998), but *G. stenostaurion* has an LAD above or co-occurs with the FAD of *C. kennedyi* in two of the five sections. *Gartnerago chiasta* has an LAD shortly above the Albian/Cenomanian boundary, but the LAD of *G. chiasta* is observed in the upper interval of Sites 137 and 547. The LAD of *Eiffellithus paragogus* and the LAD of *Zeugrhabdotus xenotus* appear at different depths throughout the section, and a relatively consistent stratigraphic position is not observed. *Cylindralithus sculptus* is stated to have an FAD in uppermost lower Cenomanian (Burnett et al., 1998), but the FAD is observed here in the lowermost Cenomanian. These discrepancies in stratigraphic position indicate that the lower Cenomanian bioevents used for the UC Zonation (Burnett et al., 1998) are not accurate, and fail to occur in the assigned order.

Unitary Associations

The initial analysis for the raw database produced 15 UAs, 24 clique cycles and 856 contradictions. Using the UA table generated in PAST, taxa that did not occur in any of the UAs were removed. This includes taxa that are endemic species or identified only to the genus level. Poor state of preservation may result in misidentification of a species resulting in what appears to be an endemic taxon that may or may not actually be more widespread. These adjustments to the dataset resulted in 18 UAs, 12 clique cycles, and 712 contradictions.

Biostratigraphic ranges of taxa are generated in UAs using FADs and LADs (Guex, 1991). Taxa that occur throughout the investigated interval are found in association with all species by definition. It is assumed that a given taxon is present even if it is not observed in that given sample. As a result, discontinuities are produced in the

data (Guex, 1991). These discontinuities can cause biostratigraphic contradictions, and ultimately, artificial UAs (Guex, 1991). Mailliot et al. (2006) coined the term "border effects" and addressed this issue by using the literature to check for known biostratigraphic ranges and eliminating any observed "border effects". A similar approach was used in the current study, in addition to removing taxa that displayed multiple discontinuities. "Multiple discontinuities" constitute approximately 50% virtual presence over the total range of a given taxon. This percentage is arbitrary and was chosen in order to reduce the number of species contradictions.

This method was repeated until the number of cycles was equal to zero. Long-ranging taxa and taxa with multiple discontinuities were again removed from the dataset. Cycles are produced when weak links exist in the dataset, such as superpositional relationship contradictions, so reduction of these cycles is essential (Guex, 1991).

Four UAs with no contradictions and no cycles were produced with a total of 15 taxa and 16 bioevents. These results are presented in a matrix, which displays the order in which the UAs occur (Guex, 1991; Fig. 6). The four UAs span the uppermost Albian, the Albian/Cenomanian boundary, the lower Cenomanian, and the basal middle Cenomanian; a total of approximately 4.7 m.y.

A matrix is also provided that shows the reproducibility of the UAs in each of the sections (Fig. 7). PAST internally reduces the reproducibility graph to a unique maximal path (Guex, 1991) and some UAs are merged in this process. Figure 7 shows UAs that are strictly identified (= real association) and occur in these sections; these UAs are indicated by the black boxes. The figure also shows suggested UAs (= virtual association) and these are indicated by the grey boxes. Merged UAs are the suggested UAs in the

reproducibility chart. Unitary associations 1 and 2 have a strong reproducibility, occurring in all 5 sections (n = 5). Unitary associations 3 and 4 have a weak reproducibility, occurring in only 2 of the 5 sections (n = 2).

Four Unitary Associations Zone assignments were produced. Species co-occurrences that characterize these zones are discussed below.

UA-Zone I

This UA is recognized by the presence of *Braarudosphaera stenorhetha, Braarudosphaera primula*, or *Hayesites albiensis*. It is important to note that *H. albiensis* occurs exclusively in this zone. Therefore, UA-Zone I can be correlated to the Subzones CC9a and UC0/BC27a. This means that UA-Zone 1 spans the uppermost Albian.

UA-Zone II

The characteristic species associations for UA-Zone II include the presence of *Calculites anfractus* or the co-occurrences of *L. dorothea*, *G. stenostaurion*, *B. africana*, or *W. britannica* and either *L. eccentricum* or *C. kennedyi*. (Figure 6). *Calculites anfractus,* whose presence is one characteristic species association for UA-Zone II, is the secondary calcareous nannofossil marker associated with the Global boundary Stratotype Section and Point (GSSP) of the Cenomanian. The absence of *H. albiensis* and the presence of both *C. anfractus and C. kennedyi* indicates that this zone spans the lowermost Cenomanian. *Calculites anfractus* has an FAD of 100.5 Ma (Kennedy et al., 2004) and *Corollithion kennedyi* has an FAD shortly after the Albian/Cenomanian boundary at 100.45 Ma (Gradstein et al., 2012), whereas *Hayesites albiensis* has an LAD

shortly before the boundary at 100.84 Ma (Gradstein et al., 2012). This assemblage is diagnostic of the lowermost Cenomanian.

This is supported by the co-occurrence of *C. anfractus, C. kennedyi, B. africana, W. britannica* and *L. eccentricum,* and the absence of *G. segmentatum*. The FAD of *G. segmentatum* marks the middle of CC9b and the base of UC2 (both zones span the lower half of the lower Cenomanian). Furthermore, *L. eccentricum* was recently found to have an FAD in the lower Cenomanian (Corbett and Watkins, 2014), which corroborates that UA-Zone II spans the lowermost Cenomanian. Therefore, UA-Zone II can be correlated to the lower half of Subzone CC9b and Zone UC1. Dashed lines are used to mark the lower boundary of this zone because *C. anfractus* and *C. kennedyi* can co-occur, indicating an age ~100.45 Ma, which is slightly younger than age of the Albian/Cenomanian boundary. It is not possible to identify the UC Subzone because the UC bioevents are not observed in UA-Zone II. For example, the LAD of *G. chiasta*, the FAD of G. *nanum*, and the LAD of *L. pseudoquadratus* do not characterize this zone. The FAD of *G. segmentatum*, which marks the base of UA-Zone III, indicates that UA-Zone II has to occur before the FAD of *G. segmentatum* (Fig. 6).

UA-Zone III

The characteristic species associations for UA-Zone III are the co-occurrence of *G. segmentatum* and either *C. alta, S. mutterlosei,* or *G. gammation* (Figure 6). This zone is characterized by the co-occurrence of *C. alta, S. mutterlosei, B. gammation, L. eccentricum, C. kennedyi, and G. segmentatum* and the absence of *L. dorotheae, G. stenostaurion, B. africana, W. britannica,* and *C. anfractus,* Therefore, UA-Zone III can be correlated to the upper half of Subzone CC9b and Zone UC2. It is not possible to

identify the UC Subzone because the UC bioevents are not observed in UA-Zone III. For example, the LAD of *Z. xenotus* and the FAD of *C. sculptus* do not occur together in UA-Zone III. The top of this zone is marked by the FAD of *L. acutus,* which has an FAD at the base of UA-Zone IV. It is assumed that the top of UA-Zone III is below the FAD of *L. acutus* (Fig. 8).

UA-Zone IV

The characteristic species association for UA-Zone IV is the presence of *L. acutus*. In addition, this zone can be recognized by the co-occurrence of *C. kennedyi, L. eccentricum, or G. segmentatum,* and the absence of *C. alta,* S. mutterlosei, and *B. gammation*. The nannofossil marker for the basal middle Cenomanian (Gradstein et al., 2012) is *L. acutus*; therefore, UA-Zone IV can be correlated to Subzone CC10a and Zone UC3. It is not possible to identify the correlative UC Subzone because the UC bioevents are not observed in UA-Zone VI, for example, the LAD of *I. compactus*, the LAD of *G. theta* and the LAD of *A. cenomanicus* do not characterize UA-Zone VI.

Ranking and Scaling (RASC) Optimum Sequence

The bioevents were ranked and scaled to produce an optimum sequence of bioevents that is summarized in Table 3. The optimum scaled sequence generated from the RASC analysis is shown in Figure 9 as bioevents plotted against their cumulative distance. One penalty point is assigned when the order of two events in the section is not the same order of these two events in the optimum sequence; therefore, an event occurring higher in the section than in the optimum sequence will be assigned a high score. A penalty point of 0 indicates the stratigraphic positions are accurate with no

discrepancies. A range of -1-1, indicates possible minor changes in the stratigraphic positions of the given bioevents, but, these bioevents are still reliable. An assignment of -3 and -4 penalty points indicates that the stratigraphic position of these bioevents are unreliable and often occur out of place. See Table 3 for the assigned penalty points for each bioevent.

This analysis indicates that other bioevents are useful for lower Cenomanian biostratigraphy, which have not been previously used in the CC (Perch-Nielsen, 1985) and UC (Burnett et al., 1998) zonations. *Braarudosphaera primula* - LAD, *Braarudosphaera africana* - LAD, *Braarudosphaera stenorheth*a - LAD, *Laguncula dorotheae* – LAD, *Gartnerago stenostaurion* - LAD, *Lithraphidites eccentricum* - FAD, *Staurolithites mutterlosei* - LAD, *Calcicalathina alta* - LAD and *Broinsonia gammation* - LAD are bioevents that are not used in these schemes. The reliability of these bioevents as lower Cenomanian markers were further investigated.

5. Discussion

DSDP Leg 14, Site 137 Age Model

Samples 137Z-8R-2, 125-126 cm through 137Z-10R-1, 102-103 cm (267.76 - 284.03 mbsf), contain abundant, poor to well-preserved nannofossil assemblages that include *Corollithion kennedyi*, *Helenea chiastia, Axopodorhabdus biramiculatus,* and *Lithraphidites acutus.* This assemblage is diagnostic of the middle Cenomanian Subzone CC10a (=UC3a).

Shipboard studies of Site 137 foraminifera by Beckmann (1972) concluded that Cores 7 (256 to 265 meters) through 15 (348 to 357 meters) and Section 1 of Core 16 are lower – upper Cenomanian (Beckmann, 1972). Roth and Thierstein (1972) and Bukry

(1972) assigned these samples to the upper Albian - Cenomanian. The bioevents observed in this study do not corroborate Beckmann's (1972) finding, and a new age model with subdivisions is proposed (Fig. 3). Samples 137Z-8R-2, 125-126 cm through 137-16R- 4, 131-132 cm (267. 76-380.82 mbsf) contain calcareous nannofossils that are diagnostic of the upper Albian - middle Cenomanian. *Lithraphidites acutus* is the nannofossil marker for the basal middle Cenomanian (Gradstein et al, 2012) and its FAD occurs in 137Z-10R-1, 102-103 cm (284.03 mbsf). The FAD of *Corollithion kennedyi* and *Lithraphidites acutus* were used to constrain the lower Cenomanian.

Another biostratigraphic discrepancy was observed in that *Planomalina buxtorfi*, a planktonic foraminifera restricted to the upper Albian occurs above the Albian/Cenomanian boundary. Petrizzo et al. (2015) also observed an LAD above the A/C boundary at Blake Nose. This finding is attributed to diachroneity of the LAD of *P. buxtorfi* and confirms that it is an unreliable regional and global marker. This lower Cenomanian LAD is also observed in Mediterranean area (Sigal, 1977), North Madagascar (Collignon et al., 1979), and Central Tunisia (Robaszynski et al., 2008).

DSDP Leg 79, Site 547 Age Model

Wiegand (1984) analyzed calcareous nannofossils in site 547 and produced an age model indicating the middle - late Cenomanian is present in this section. A subsequent study by Nederbragt et al. (2001) concluded that Cores 40 (431 mbsf) through 64 (659.28 mbsf) are uppermost Albian and lower Cenomanian, including the Albian/Cenomanian Boundary at approximately 628 mbsf. This current study corroborates the Nederbragt et al. (2001) overall age model.

Corollithion kennedyi has an FAD at 542.13 mbsf, indicating an expanded section across the A/C boundary. This difference in stratigraphic position is attributed to possible varying taxonomic definitions for this taxon. *Corollithion kennedyi* has a characteristic crossbar in the central area that is optically split in the light microscope (LM) (Crux, 1981). A transitional morphotype between *C. signum* and *C. kennedyi* is observed in this section close to the Albian/Cenomanian boundary. One specimen was observed at 659.28 mbsf, it was absent until 619.9 mbsf, where 3 specimens where observed. These transitional morphotypes are referred to as *Corollithion* sp. cf. *C. kennedyi* in this study. These transitional morphotypes exhibit a thick central crossbar and a more hexagonal shape, similar to that of *C. kennedyi*. This morphotype lacks optically split crossbars; however, this indicates that this is not *C. kennedyi*. If Nederbragt et al. (2001) identified these transitional morphotypes as *C. kennedyi*, this would explain the apparent discrepancy in their placement of the FAD at approximately 628 mbsf in their study. Plate 1 (photos 13 – 16) shows the differences between *C. kennedyi* and *Corollithion* sp. cf. *C. kennedyi.* In these photos, it is evident that the *C. kennedyi* bar is more complex than that of the transitional morphotype.

UA and RASC Comparisons

Four unitary associations zone assignments were produced and 16 bioevents were identified using RASC. Figure 11 shows the dendrogram produced by scaling, to which the UA Zones are being compared. A total of six clusters were identified on the scaling dendrogram.

Cluster 1 is distinct and can be separated easily from the other zones. *Braarudosphaera primula* - LAD, *Hayesites albiensis* - LAD *and Braarudosphaera*

stenorhetha - LAD form a cluster of datums and occur exclusively in this zone, which can be correlated to UA-Zone I. UA-Zone I is recognized by the presence of *Braarudosphaera stenorhetha, Braarudosphaera primula* or *Hayesites albiensis*. *Hayesites albienis* exclusively occurs in both zones.

It is more difficult to discern bioevents that co-occur in Clusters 2-5. Clusters 2 - 5 correspond to UA-Zones II and III. In Clusters 2 and 3, *Calculites anfractus* - FAD, *Laguncula dorotheae* - LAD, *Gartnerago stenostaurion* - LAD, *Braarudosphaera* africana - LAD, *Calculites anfractus* - LAD, *Lithraphidites eccentricum* - FAD, *Corollithion kennedyi* - FAD and *Watznaueria britannica* - LAD co-occur; these clusters are correlated to UA-Zone II. In Clusters 4 and 5, *Staurolithites mutterlosei* - LAD and *Gartnerago segmentatum* - FAD, *Calcicalathina alta* - FAD and *Broinsonia gammation* - LAD co-occur; these clusters are correlated to UA-Zone III. Cluster 6 can be correlated to UA-Zone IV, for which the characteristic species association is the presence of *L. acutus*.

With the exception of single UA bioevents, such as *Braarudosphaera primula* - LAD, *Hayesites albiensis* - LAD *and Braarudosphaera stenorhetha* - LAD, *Calculites anfractus* - FAD/LAD and *Lithraphidites acutus* - FAD, most of the bioevents occur in more than one UA zone, which is described as "overlapping" (Agterberg, 1990). Overlapping bioevents follow a similar pattern to that of the clusters, which indicates that the UA Zones are similar to the optimum sequence produced by RASC (Fig. 9). The only discrepancy is that *Gartnerago segmentatum* - FAD belongs to UA-Zone IV, yet, it occurs before *Lithraphidites acuctus* - FAD. This can be attributed to the scarcity and

uncertainties in the true FAD of *Gartnerago segmentatum*. These relationships are shown in Fig. 9.

The UA and RASC methods correlate well, regardless of being deterministic and probabilistic methodologies, respectively. These correlations indicate that the biostratigraphic schemes proposed for the lower Cenomanian are reproducible and reliable.

Reliability Indices

The results of the reliability indices for DSDP sites 137 and 547 are presented in Tables 4 and 5. According to Bralower et al. (1988), all the calculated values for Sites 137 and 547 are considered to have very low reliability indices given that values for Cenozoic species exhibit average values of 20 or more. For Site 137, reliability index values could only be calculated for *Lithraphidites eccentricum* and *Staurolithites mutterlosei*, each yielding a value of 0.165 and for Site 547, *Corollithion kennedyi, Gartnerago stenostaurion* and *Staurolithites mutterlosei*, each being assigned a value of 0.09. The two methods presented by Bergen et al. (2013) used semi-quantitative data, as a result, it is difficult to rank the values on a basis of a "Strong to Weak".

For the proposed binomial probabilities method, values were calculated for DSDP sites 137 and 547. An arbitrary rating scale was assigned to the reliability index values. "Strong" reliability values range from 13.02 – 14.78, "Moderate" reliability index values range from 9.43 – 11.98, and "Weak" reliability index values range from 1.99 – 6.20 (Tables 4 and 5).

It is important to note that Site 137 has a condensed interval at 347.71 mbsf where *Corollithion kennedyi* - FAD, *Discorhabdus watkinsii* – FAD, *Gartnerago*

stenostaurion - LAD, *Gartnerago chiasta* – LAD, *Lithraphidites eccentricum* - FAD *and Watznaueria britannica* – LAD bioevents are observed. A condensed section can potentially affect the full stratigraphic range for a given taxon; however, the binomial probability method allows for reliability index values to be calculated in such sections. The Bralower et al. (1988) method requires high-resolution sampling and spacing through an expanded section and cannot be applied to sections with condensed intervals. *Gartnerago stenostaurion, Lithraphidites eccentricum* and *Staurolithites mutterlosei* are species that occur consistently through their stratigraphic range, and can serve as reliable markers for lower Cenomanian biostratigraphy.

Other Findings and Implications for Lower Cenomanian Biostratigraphy

In addition to bioevents derived from the quantitative biostratigraphic analysis, other bioevents were identified in this study that appear to have biostratigraphic significance in the lower Cenomanian. These bioevents were recorded as having different age ranges when compared to the assigned type levels, UC/CC Zonation schemes and/or the geologic time scale. Note that the LAD of *Gartnerago stenostaurion*, LAD *Gartnerago chiasta,* FAD *Discorhabdus watkinsii and the* LAD *Watznaueria britannica* are not discussed in the context of Site 137. This is because these bioevents occur simultaneously in a condensed interval in this section; therefore, this does not allow for the true order of events to be observed.

According to the UC Zonation, the LAD of *Gartnerago stenostaurion* is placed in Subzone UC0b, which is equivalent to the upper Albian. In this study, *G. stenostaurion* has its FAD in the lower Cenomanian. The LAD of *G. stenostaurion* almost coincides with the LAD of *Gartnerago chiasta* (99.94 Ma [Gradstein et al., 2012]). An early

Cenomanian extinction also corroborates Hill's (1976) finding in which *G. stenostaurion* was assigned a type level of middle Albian - lower Cenomanian. Watkins et al. (2005) estimated that *G. stenostaurion* has an LAD of 99.73 Ma indicating an early Cenomanian extinction. Bown (2005) also reported a mid-Albian (upper Zone NC8) to lower Cenomanian (Zone UC1/UC2) at Sites 1207, 1213 and 1214 (Leg 198, Shatsky Rise).

For Sites 137 and 547, the LAD of *Lithraphidites alatus* occurs in the lower Cenomanian. *Lithraphidites alatus* was assigned a Cenomanian type level, but no subdivisions were indicated (Thierstein, 1972). Therefore, it is plausible that *L. alatus* had an early Cenomanian extinction and can be used as a zonal marker.

Discorhabdus watkinsii was described as a rare species restricted to the Cenomanian section in the Bounds core, western Kansas; it was assigned an upper Cenomanian type level (Bergen, 1998). In this study, *D. watkinsii* was observed in multiple samples for both localities, which suggests that *D. watkinsii* may not be as rare as previously believed, and in fact, its FAD can be used as an early Cenomanian zonal marker for regions such as the western proto-North Atlantic Ocean.

Staurolithites mutterlosei is a morphologically distinct species with LAD in the lower Cenomanian. The species was assigned a Hauterivian – Barremian range by Crux (1989), but the present study places the LAD of *S. mutterlosei* in the lower Cenomanian. Watkins et al. (2005) corroborates this finding, as the LAD of *S. mutterlosei* is observed after the FAD of *C. kennedyi* (100.45 Ma [Gradstein et al., 2012]).

The FAD of *Cylindralithus sculptus* is in the lower Cenomanian, before the assigned age of 97.31 Ma (Gradstein et al., 2012). For example, at both DSDP sites 137 and 547, *C. sculptus* has an FAD below that of *C. kennedyi* (100.45 Ma [Gradstein et al.,

2012]) (Table 2). *Cylindralithus sculptus* has also been shown to be a poor marker based on the calculated reliability index.

The range of *Zeugrhabdotus xenotus* in this study supports the idea that the subzone between the LAD of *Z Zeugrhabdotus xenotus* and the FAD of *C. sculptus* cannot be identified in oceanic sequences (Gradstein et al., 2012). In addition to the problems associated with the FAD of *C. scultpus* in this study, *Z. xenotus* co-occurs with *C. sculptus* at both localities, indicating that Subzone UC2b of Burnett et al. (1998), based on the interval between the LAD of *Z. xenotus* and the FAD of *C. sculptus*, is not valid, as their co-occurrence violates the definition of the subzone. At Site 137, *Z. xenotus* also co-occurs with *L. acutus*, a species that marks the base of the middle Cenomanian (96.16 Ma [Ogg and Hinnov, 2012]). This implies that *Z. xenotus* may have gone extinct later than previously believed, or the LAD is diachronous. Because the middle - upper Cenomanian is not present at all the localities used in this study, the absolute LAD cannot be determined. With these findings, it is necessary to revisit the biostratigraphic significance of Z. *xenotus* in the lower Cenomanian.

Calculites anfractus as a proposed GSSP Secondary Calcareous Nannofossil Marker for the Basal Cenomanian

The FAD of *Calculites anfractus* was designated as a secondary calcareous nannofossils marker for the basal Cenomanian (Kennedy et al., 2004). However, *Calculites anfractus* is not a reliable marker as it is very rare, with only 4 specimens found between 630.51 and 619.9 mbsf at Site 547. The genus *Calculites* is a holococcolith, representing the coccolithophore haploid phase of the life cycle, and have skeletons comprised of numerous minute (<0.1 μm) crystallites that are all of similar

shape and size. Holococcoliths do not occur in all oceanic settings and are more susceptible to dissolution than heterococcoliths.

Sites used in this study are both located off the west coast of North Africa, however, there is a noticeable difference in species diversity between the two sites. At Site 547, a total of 11 holococcolith species were identified; this excludes specimens that were only identified to the genus level. At Site 137, a total of 2 holococcolith species were identified. While both of these sites are located in similar latitudes, the geological and paleoceanographic settings are different. Site 137 was drilled at a water-depth of 5361 meters and recovered an upper Albian through the lowermost upper Cenomanian section characterized by nannofossil marl to chalk ooze deposited in an area virtually free of terrigenous influx (Leg 14 Shipboard Scientific Party, 1972). Site 547 was drilled at a water-depth of 3940.5 meters and recovered a sediment sequence interpreted to have been deposited on the continental slope at mid-bathyal depth. The average rate of sediment accumulation was about 29 m/m.y. (Winterer and Hinz, 1984). Higher holococcolith abundance and diversity could result from greater terrigenous input, and/or higher sediment accumulation rates, which led to exceptional preservation of the nannofossil assemblage. In addition, deposition at Site 137 presently located approximately 1421 meters deeper than Site 547, likely occurred at greater paleodepth where dissolution would be higher. These potential controls on the distribution and preservation of holococcoliths makes *C. anfractus* an unreliable marker for the base of the Cenomanian.

Biostratigraphic Significance of *Lithraphidites eccentricum*

Watkins and Bowdler (1984) first described *L. eccentricum* as a subspecies of *L. acutus* from a middle Cenomanian sample from DSDP Site 540 (Gulf of Mexico). *Lithraphidites acutus* marks the base of Zones CC10 and UC3, which are basal middle Cenomanian. *Lithraphidites eccentricum* was believed previously to have an FAD in the middle Cenomanian because it was assigned an age based on its co-occurrence with planktonic foraminifera from the *Rotalipora cushmani* Zone and *Rotalipora appenninica* Subzone; these foraminiferal assemblages are diagnostic of the middle Cenomanian (Premoli Silva and McNulty, 1984). However, a taxonomic review later showed that the FAD of *L. eccentricum* co-occurs with foraminifer *Hedbergella libyca* (Premoli Silva and McNulty, 1984) (= *Paracostellagerina libyca* Georgescu and Huber, 2006); however this taxon went extinct shortly after the Albian/Cenomanian boundary. This indicates that *Lithraphidites eccentricum* has a FAD in the early Cenomanian, which is supported by the position of the FAD of *L. eccentricum* at TDP Site 24 (Ando et al., 2015). The present study corroborates this finding as the FAD of *L. eccentricum* is observed at 594.13 mbsf in sample 547A-57-2, 12-13 cm, 52 meters below the FAD *C. kennedyi*, which indicates an FAD in the lower Cenomanian.

Comments on *Gartnerago segmentatum*

Gradstein et al. (2012) use the LAD of *Gartnerago chiasta* (99.94 Ma [Gradstein et al., 2012]) and the FAD of *Gartnerago segmentatum* (98.26 Ma [Gradstein et al., 2012]) as marker taxa for the lower Cenomanian. *Gartnerago segmentatum* also marks the base of Zone UC2 (Burnett et al., 1998). In this study, *G. chiasta* occurs consistently through both sites, disappearing before the FAD of *G. segmentatum*; however,

Gartnerago segmentatum is very rare in both sites examined here with only two specimens observed at Site 137 and one specimen at Site 547.

The low abundance of *Gartnerago segmentatum* appears to be controlled by paleoceanographic and regional conditions (Hardas et al., 2012). At Shatsky Rise (Hole 1207B, ODP Leg 198) the FAD of *G. segmentatum* was observed higher than expected, as a result, Subzones UC2c–UC1b could not be differentiated (Lees and Bown, 2005), while it was observed in the Middle Cenomanian Event (MCE) at Demerara Rise (Site 1260, ODP Leg 207, Hardas et al., 2012). This indicates that *G. segmentatum* may have a diachronous FAD and should only be used as a regional, rather than a global marker. Mosher et al. (2006) described local paleoceanographic events at Demerara Rise that affected evolution of the *Gartnerago* genus.

6. Conclusions

Four Unitary Associations Zones and sixteen bioevents for the upper Albian-lower Cenomanian were generated using RASC optimum sequencing. From this sequence, in conjunction with binomial probability reliability index calculations, *Gartnerago stenostaurion*, *Lithraphidites eccentricum* and *Staurolithites mutterlosei* were identified as strong reliable markers for lower Cenomanian biostratigraphy. These markers are morphologically distinct and occur consistently through their stratigraphic ranges. A comparison of the UA and RASC results indicates that these methods (deterministic and probabilistic, respectively) produce similar results. Overlapping of these bioevents in Clusters 2 -5 also follows a similar pattern produced by the UAs.

The proposed Reliability Index from this current study is a viable option for assessing the Mesozoic marker species. Bralower et al's. (1988) method produced low

values for Mesozoic taxa because the method is designed for high-resolution sampling, a scale not feasible here due to patchy abundance and distribution of Mesozoic marker species (Bralower et al., 1988). The binomial probability method and the associated reliability index values should be used for Mesozoic taxa because this method produces a reasonable range of values that can also be used in condensed intervals.

The validity of the CC (Perch-Nielsen, 1985) and UC (Burnett et al., 1998) zonations is confirmed because the above methods produce a similar zonation scheme; however, the CC Zones of Perch-Nielsen (1985) lack the biostratigraphic resolution produced herein. *Braarudosphaera primula* - LAD, *Braarudosphaera stenorhetha* – LAD and *Hayesites albiensis* – LAD are bioevents that can be used to improve the resolution of Zone CC9a. *Calculites anfractus* - LAD, *Laguncula dorotheae* - LAD, *Gartnerago stenostaurion* - LAD, *Braarudosphaera africana* - LAD, *Calculites anfractus* - LAD, *Lithraphidites eccentricum* - FAD, *Watznaueria britannica* – LAD, *Staurolithites mutterlosei* - LAD, *Gartnerago segmentatum* - FAD, *Calcicalathina alta* - LAD and *Broinsonia gammation* - LAD are bioevents that can improve the resolution of Zone CC9b. Some of the UC Zonation Subzones (Burnett et al., 1998) cannot be recognized easily. For example, it is not possible to split Zone UC1 because the LAD of *Gartnerago chiasta*, the FAD of Gartnerago *nanum*, and the LAD of *Lithraphidites pseudoquadratus* do not characterize any of the zones produced in this study. In addition, the LAD of *Zeugrhabdotus xenotus* co-occurs with *Cylindralithus sculptus* at sites 137 and 547, indicating that Subzone UC2b of Burnett et al. (1998), based on the interval between the LAD of *Z. xenotus* and the FAD of *C. sculptus*, is not valid, as their co-occurrence violates the subzone definition.

Other species are suggested markers for the lower Cenomanian in the proto-North Atlantic Ocean. Watkins and Bowdler (1984) first described subspecies of *Lithraphidites eccentricum* as a subspecies of *Lithraphidites acutus* and assigned a middle Cenomanian age. *Lithraphidites acutus* marks the base of Zones CC10 and UC3 from the basal Cenomanian. *Lithraphidites eccentricum* was assigned an early Cenomanian age based on co-occurrence with planktonic foraminiferal assemblages of the *Rotalipora cushmani* Zone and *Rotalipora appenninica* Subzone. A taxonomic review later showed that the FAD of *L. eccentricum* co-occurs with *Hedbergella libyca*, a foraminiferal species that went extinct shortly above the Albian/Cenomanian boundary, suggesting that *L. eccentricum* has an FAD in the lower Cenomanian. This study corroborates these findings as *Lithraphidites eccentricum* was noted above the Albian/Cenomanian boundary, with a FAD occurring before the FAD of *C. kennedyi* at Site 547. Other significant bioevents include the LAD of *Lithraphidites alatus* and the FAD of *Discorhabdus watkinsii.* These observations are not based on statistical methods; as a result, these bioevents need to be further explored.

Because holococcoliths are poorly understood and restricted by depositional environment and paleoceanographic settings, they are not reliable primary markers and should not be used to represent global events. For example, only four specimens of *Calculites anfractus* were noted between 630.51 and 619.9 mbsf at Site 547. Therefore, *C. anfractus* cannot serve as a global basal marker for the Cenomanian.

New biostratigraphic information revises the age models for DSDP Site 137, by identifying an upper Albian interval, and for Site 547 with the recognition of an expanded

Albian/Cenomanian boundary section, based on the FAD of *C. kennedyi*. These results advance the mid-Cretaceous biostratigraphic framework for future work.

7. Taxa List for Taxa Discussed in this Study

Braarudosphaera africana Stradner, 1961

Braarudosphaera primula Black, 1973

Braarudosphaera stenorhetha Hill, 1976

Broinsonia gammation Hill, 1976

Calcicalathina alta Perch-Nielsen, 1979

Calculites anfractus (Jakubowski, 1986) Varol & Jakubowski, 1989

Corollithion kennedyi Crux, 1981

Cylindralithus sculptus Bukry, 1969

Discorhabdus watkinsii Bergen *in* Bralower & Bergen, 1998

Eiffellithus paragogus Gartner *in* Robaszynski et al. (1993)

Gartnerago chiasta Varol, 1991

Gartnerago segmentatum (Stover, 1966) Thierstein, 1974

Gartnerago theta (Black, 1959) Jakubowski, 1986

Gartnerago stenostaurion Hill, 1976

Hayesites albiensis Manivit, 1971

Laguncula dorotheae Black, 1971

Lithraphidites acutus subsp. *acutus* Verbeek & Manivit *in* Manivit et al., 1977

Lithraphidites alatus subsp. *alatus* Thierstein *in* Roth & Thierstein, 1972

Lithraphidites eccentricum (Watkins *in* Watkins and Bowdler 1984) Corbett & Watkins, 2014

Staurolithites mutterlosei Crux, 1989

Watznaueria britannica, (Stradner, 1963) Reinhardt, 1964

Zeugrhabdotus xenotus (Stover, 1966) Burnett *in* Gale et al., 1996

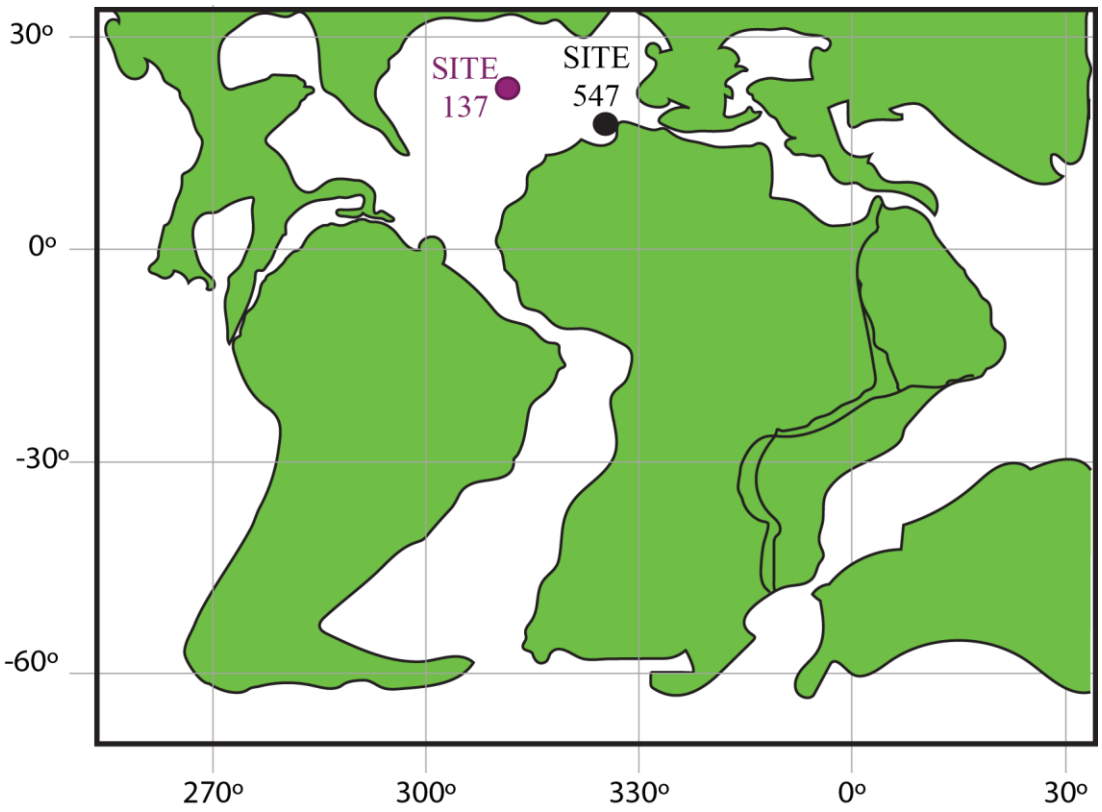

Fig.1. Paleogeographic reconstruction of the Cenomanian (100.5 Ma) modified from Ocean Drilling Stratigraphic Network (ODSN) plate tectonic reconstruction.

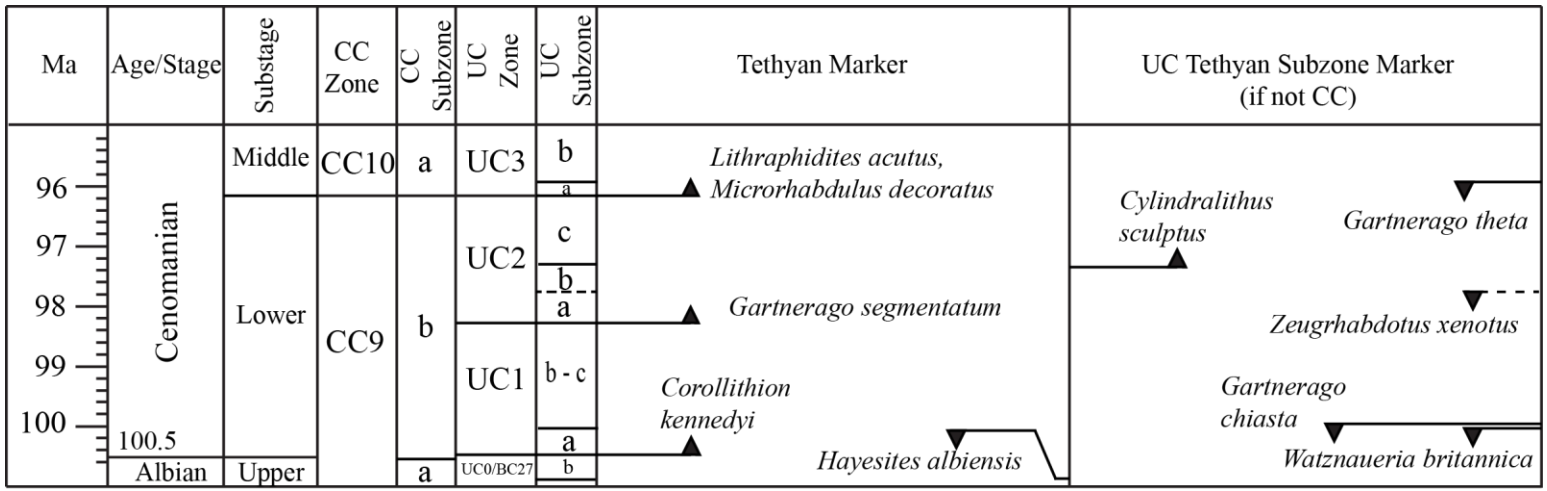

Fig. 2. Comparison of the CC (Perch-Nielsen, 1985) and UC (Burnett et al., 1998) Zonation schemes.

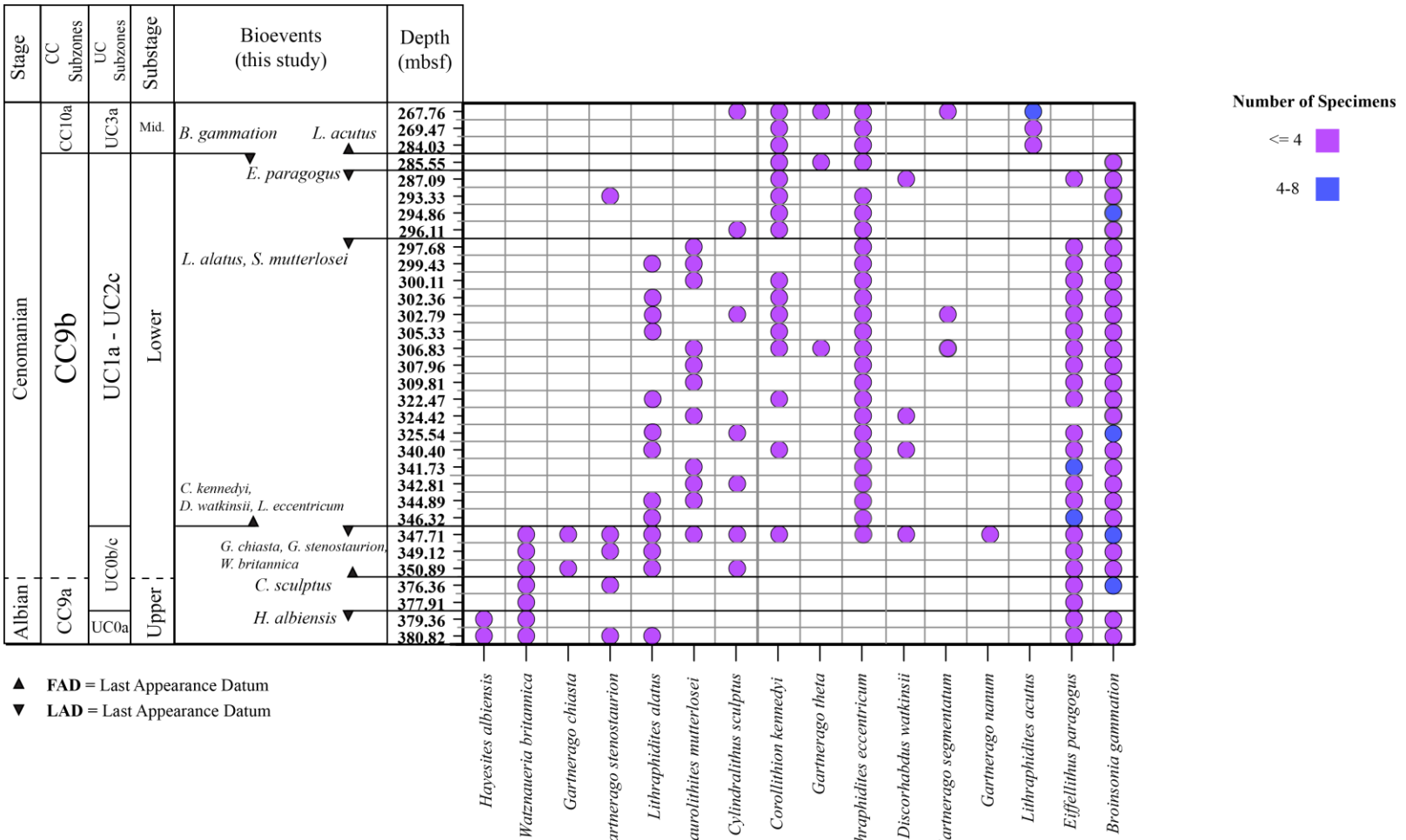

Fig. 3. Bioevents identified at DSDP Site 137.

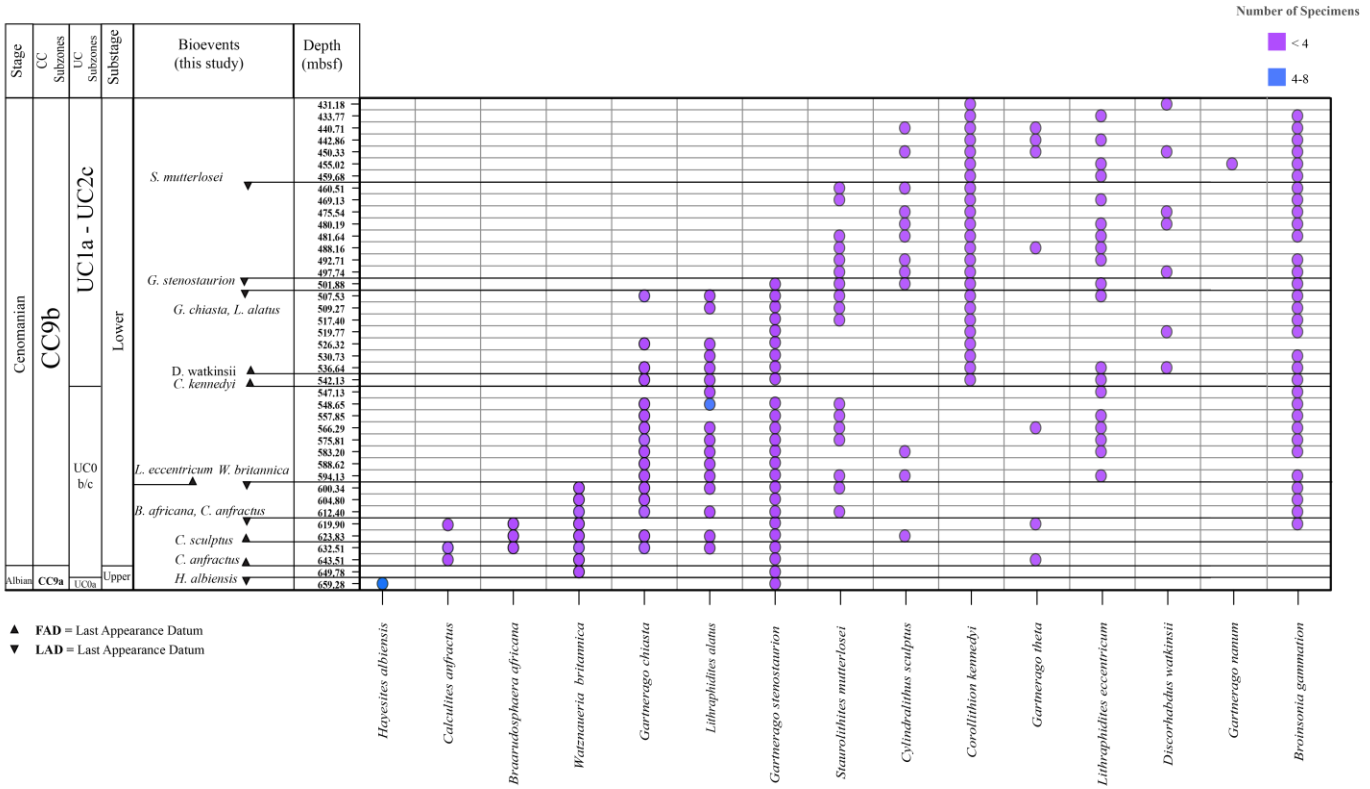

Fig. 4. Bioevents identified at DSDP Site 547.

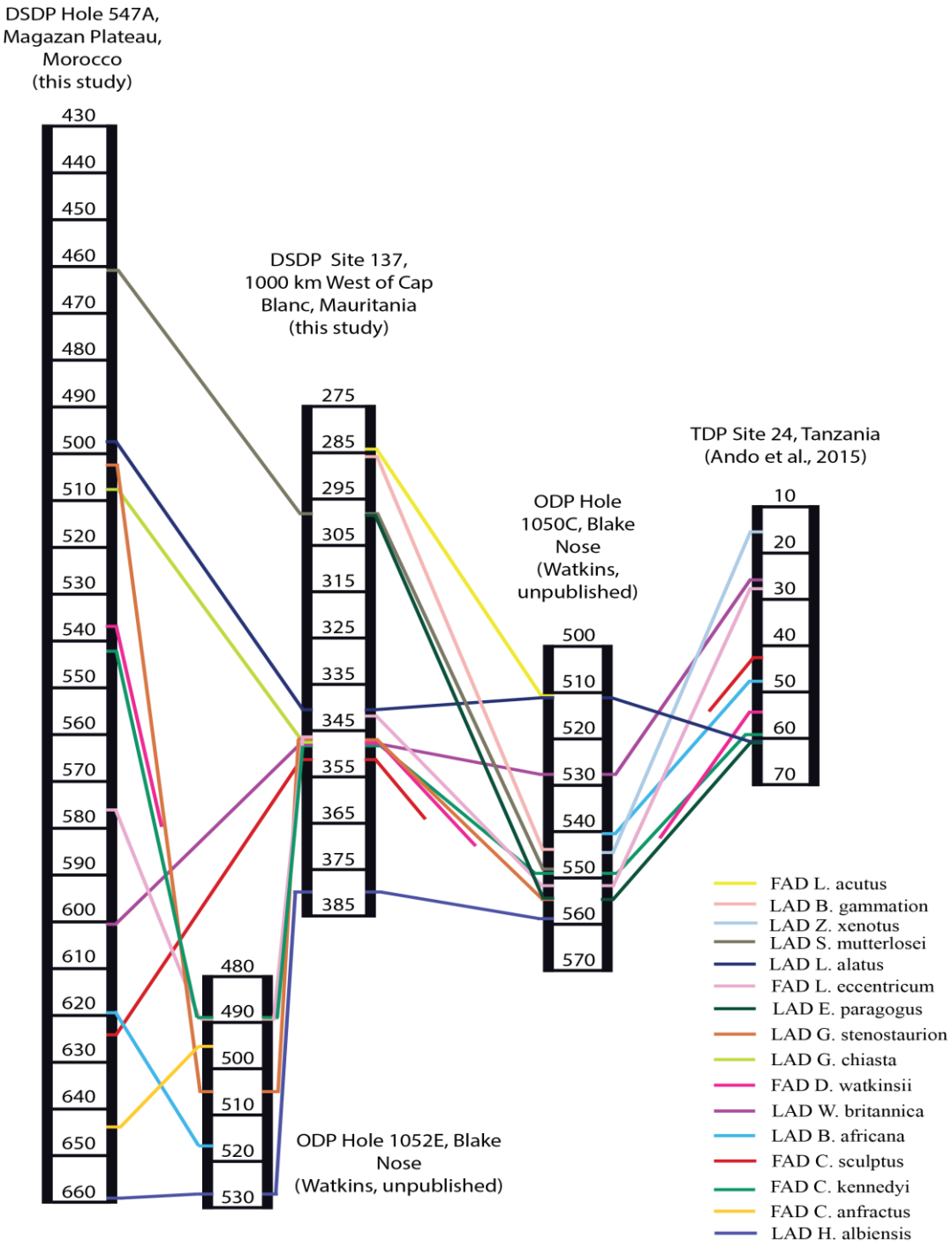

Fig. 5. Crossplot diagram correlating bioevents between DSDP sites547 and 137, ODP holes 1050C and 1052E, and TDP Site 24. The numbers are depth in meters below sea floor (mbsf).The light red line representing the LAD of *Cylindralihtus sculptus* and the dark pink line representing the FAD of *Discorhabdus watkinsii* are discontinuous because these bioevents could not be traced through all the sections. In this case, the FAD of D*iscorhabdus watkinsii* at holes 1050C and 1052E occurs before the LAD of *Hayesites albiensis*, while this superpositional relationship is not observed in the other sections.

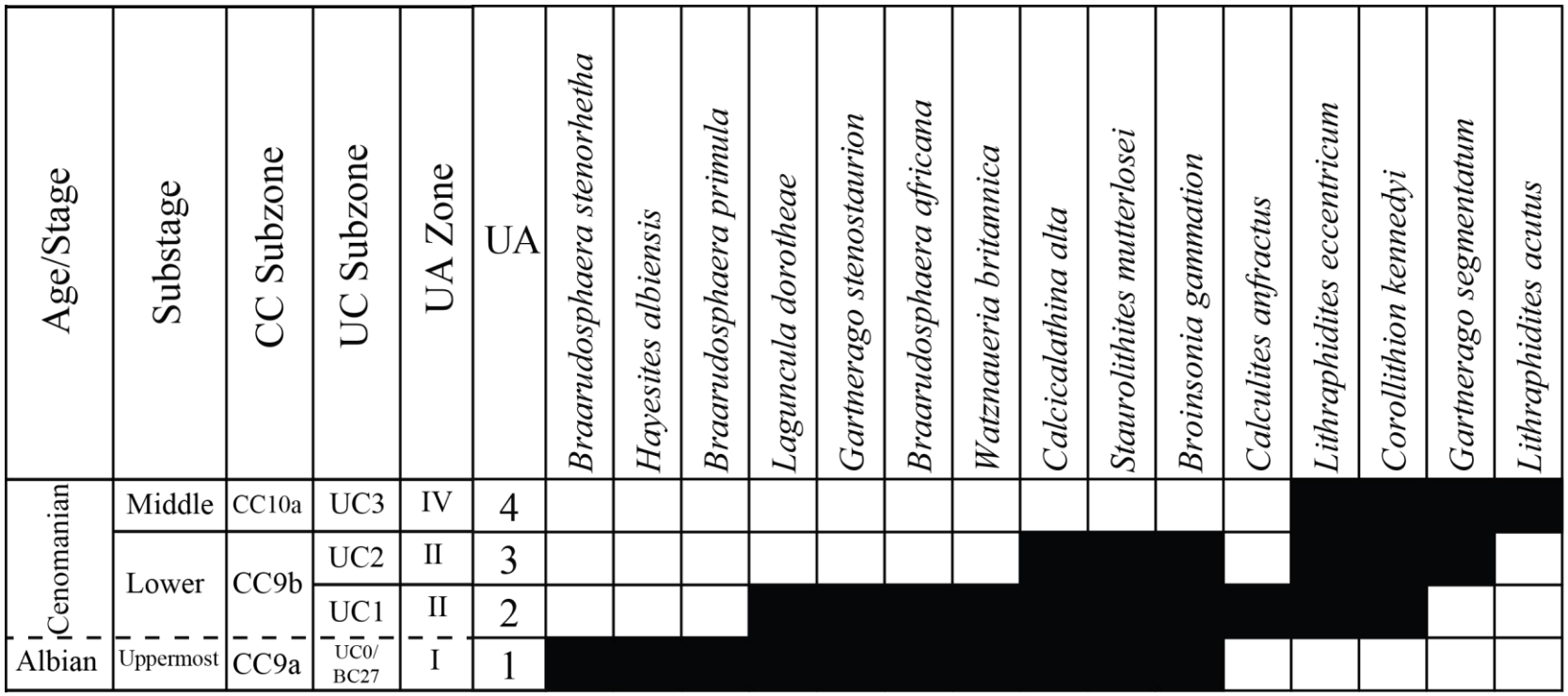

Fig. 6. Unitary Associations Zones and associated bioevents. The black boxes indicate species that can occur in the given zone.

UA - Zone	UA	DSDP Hole 547A, Magazan Plateau, Morocco (this study)	DSDP Site 137, 1000 km West of Cap Blanc, Mauritania (this study)	ODP Hole 1050C, Blake Nose (Watkins, unpublished)	ODP Hole 1052E, Blake Nose (Watkins, unpublished)	TDP Site 24, Tanzania (Ando et al., 2015)	n
IV	4						2
III	3						2
II	2						5
I	1						5

UAs that are strictly identified
Potentially identified UAs

Fig. 7. Sections in which Unitary Associations I-IV Zones are observed.

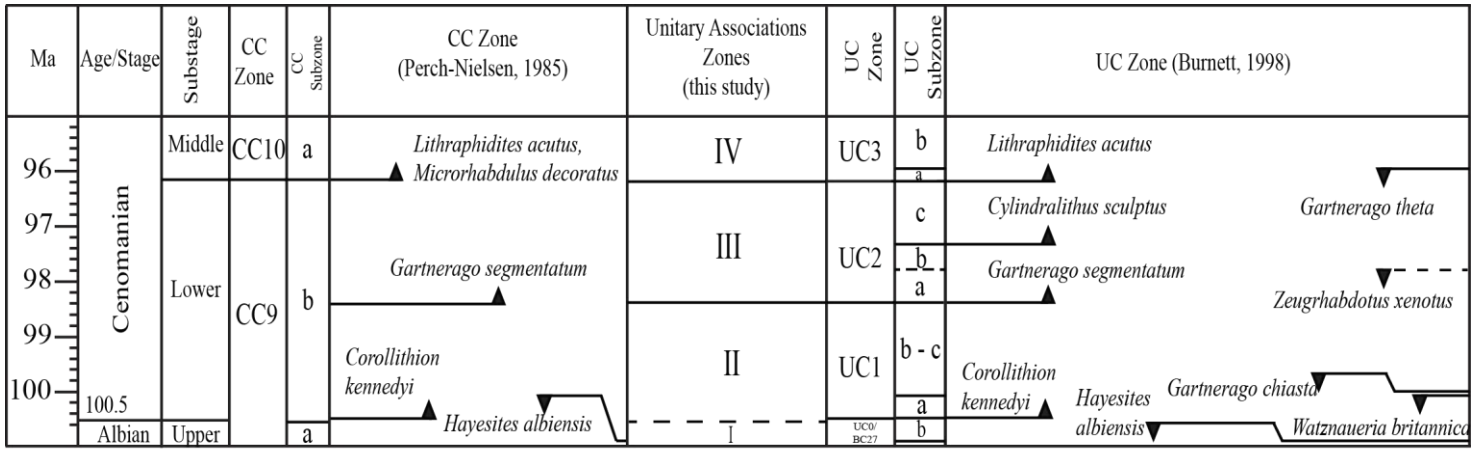

Fig. 8. Unitary Associations Zones compared to the CC Zonation (Perch-Nielsen, 1985) and UC Zonation (Burnett et al., 1998) schemes.

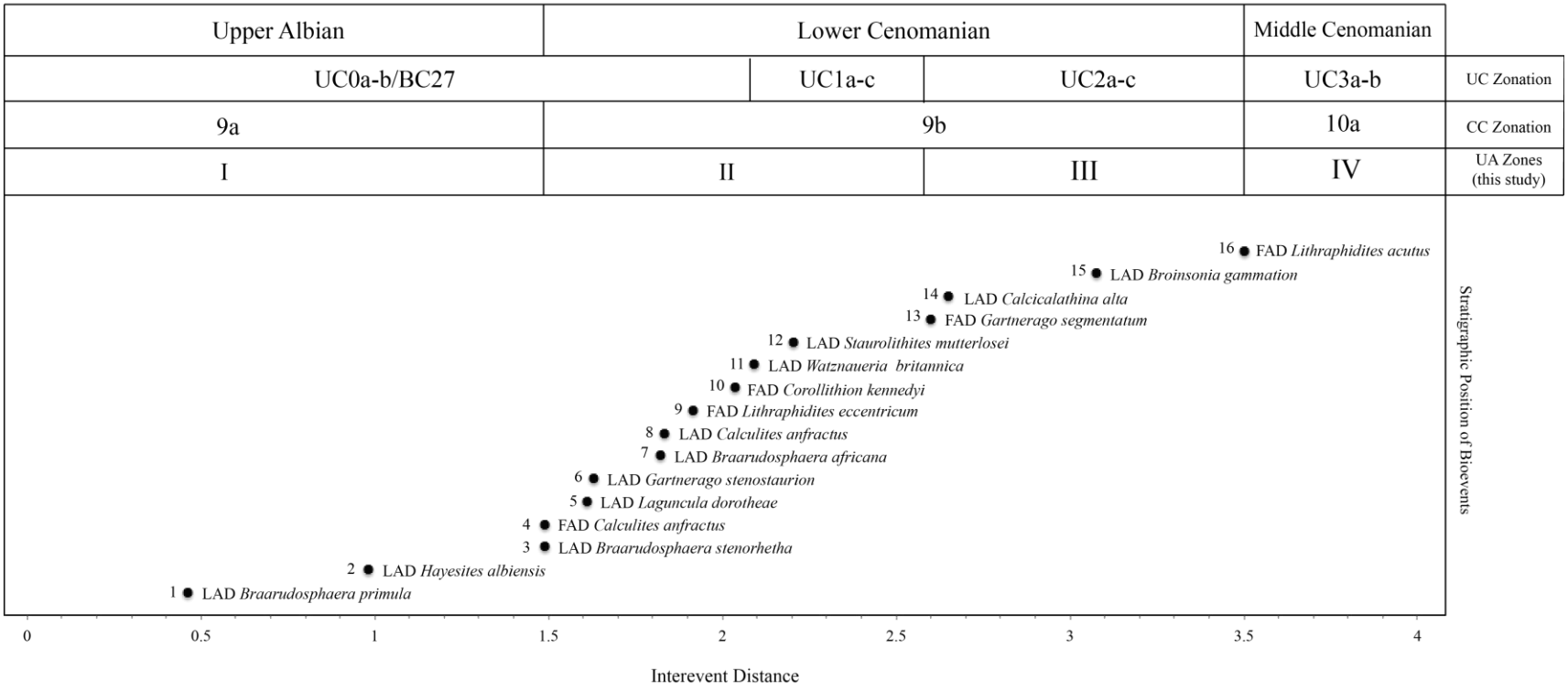

Fig. 9. Optimum sequence of events produced by scaling. Each bioevent was plotted against its interevent depth. Each number represents the stratigraphic position of the bioevent.

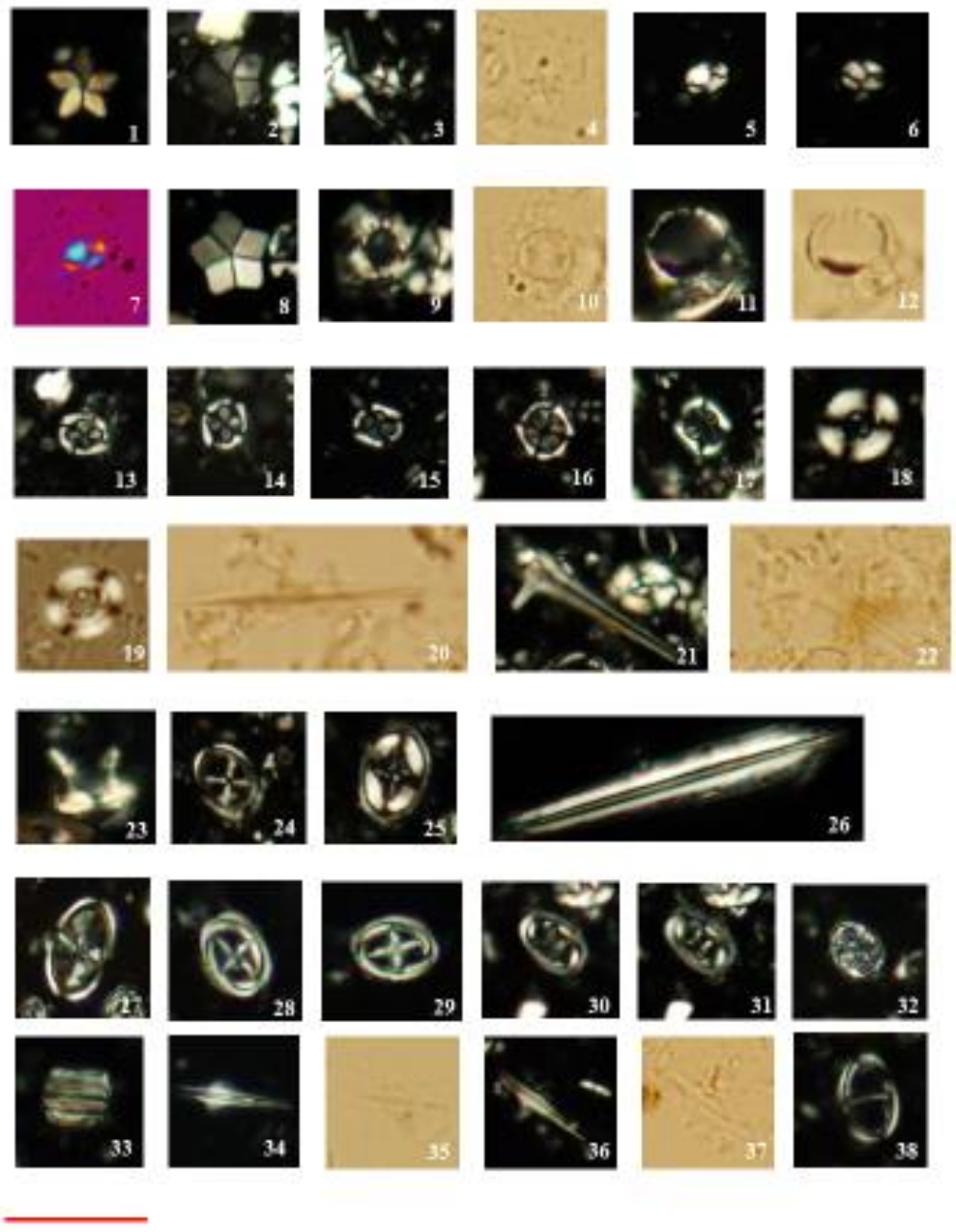

Figure 10**.** Photos 1-3, 5-6, 8-9, 11, 13-18, 21, 23-34, 36, and 38 were taken in cross-polarized light (XPL). Photos 4, 10, 12, 19, 20, 22, 35 and 37 were taken in plane-polarized light (PPL). Photo 7 was taken using a one-quarter λ gypsum plate under crossed-polarized light. The magnification is 2000x. Scale bar = 10 mm.

1. *Braarudosphaera stenorhetha* Sample 547A-64-1, 27.5-29 cm. **2.** *Braarudosphaera primula* Sample 547A-64-1, 27.5-29 cm. **3, 4.** *Hayesites albiensis* Sample 547A-64-1, 27.5-29 cm. **5-7**. *Calculites anfractus* Sample 547A-62-3, 50-51 cm **8.** *Braarudosphaera africana* Sample 547A-59-6, 8-9 cm. **9, 10**. *Cylindralithus sculptus* Sample 137-14R-6, 120-121 cm. **11, 12.** *Laguncula dorotheae* Sample 137-14R-6, 120-121 cm. **13, 14.** *Corollithion* sp. cf. *C. kennedyi* Sample 547A-59-6, 8-9 cm (13); Sample 547A-58-3, 78-80 cm (14). **15-17**. *Corollithion kennedyi* Sample 547A-51-4, 112-113 cm (15); Sample 137-9R-3, 146-147 cm (16); Sample 137-8R-2, 125-126 cm (17). **18, 19.** *Watznaueria britannica* Sample 137-16R-3, 135-136 cm. **20-22.** *Lithraphidites eccentricum* Sample 137-8R-2, 125-126 cm. **23.** *Discorhabdus watkinsii* Sample 547A-47-3, 137-138 cm. **24.** *Gartnerago chiasta* Sample 547A-53-3, 34-35 cm. **25.** *Eiffellithus paragogus* Sample 137-14R-4, 138-139 cm. **26.** *Lithraphidites alatus* Sample 547A-60-3, 32.5-34 cm. **27.** *Gartnerago stenostaurion* Sample 547A-57-6, 33-34 cm. **28, 29**. *Staurolithites mutterlosei* Sample 547A-47-3, 137-138 cm. **30, 31.** *Zeughrabdotus xenotus* Sample 137-14R-6, 120-121 cm. **32, 33**. *Calcicalathina alta* Sample 547A-59-6, 8-9 cm. **34-37**. *Lithraphidites acutus* Sample 137-9R-3, 146-147 cm (34, 35); Sample 137-8R-2, 125-126 cm (36, 37). **38.** *Gartnerago theta* Sample 547A-54-2, 78-79 cm.

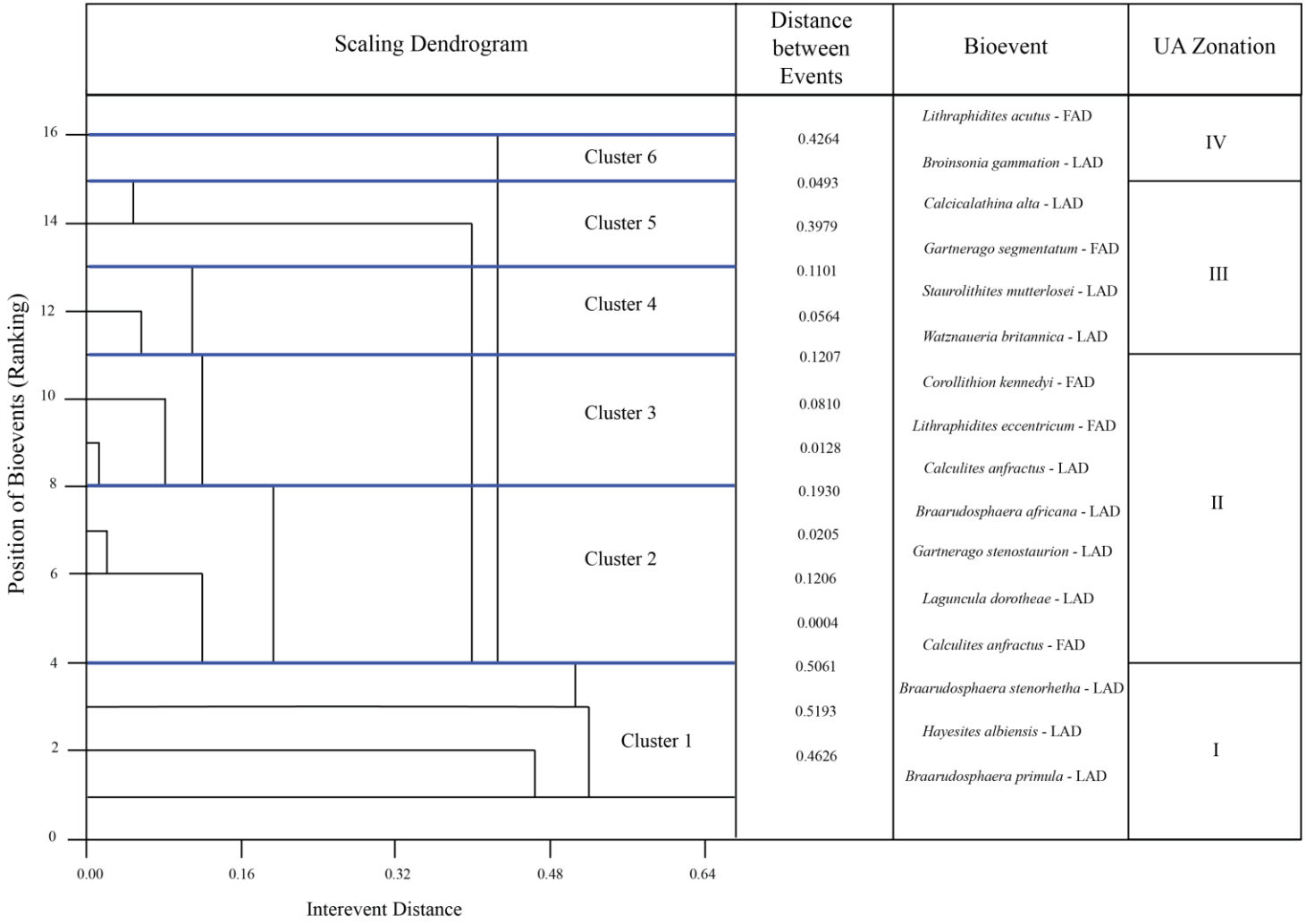

Fig. 11. Comparison of UA-Zones I-IV (current study) to the scaling dendrogram produced from RASC. Cluster 1 correlates to UA-Zone I, Clusters 2 and 3 correlate to UA-Zone II, Clusters 4 and 5 correlate to UA-Zone III and Cluster 6 correlates to UA-Zone IV.

Bioevent	DSDP Hole 547A, Magazan Plateau, Morocco (this study)	DSDP Site 137, 1000 km West of Cap Blanc, Mauritania (this study)	ODP Hole 1050C, Blake Nose (Watkins, unpublished)	ODP Hole 1052E, Blake Nose (Watkins, unpublished)	TDP Site 24, Tanzania (Ando et al., 2015)
FAD *Lithraphidites acutus*		284.03	510.4		
LAD *Broinsonia gammation*		285.55	544.05		
LAD *Zeughrabdotus xenotus*			544.05		15.08
LAD *Staurolithites mutterlosei*	460.51	297.68	548.95		
LAD *Lithraphidites alatus*	497.74	340.4	510.4		60.58
LAD *Eiffellithus paragogus*		287.09	554.79		60.58
LAD *Gartnerago stenostaurion*	501.88	347.71	554.79	504.32	
LAD *Gartnerago chiasta*	507.53	347.71			
FAD *Discorhabdus watkinsii*	536.64	347.71			54.38
FAD *Lithraphidites eccentricum*	575.81	347.71	551.02	489.08	27.31
LAD *Watznaueria britannica*	600.34	347.71	527.3		25.46
LAD *Braarudosphaera africana*	619.9		540.6	516.57	47.51
FAD *Corollithion kennedyi*	542.13	347.71	548.95	489.08	59.66
FAD *Cylindralithus sculptus*	623.83	350.89			41.98
FAD *Calculites anfractus*	643.51			494.08	
LAD *Hayesites albiensis*	659.28	379.36	558.72	526.8	

Table 1. Depths (in mbsf) of bioevents for DSDP sites and 137137, ODP holes 1050C & 1052E, and TDP Site 24. Blank cells indicate that the corresponding bioevent was not observed in that section.

Chronological order of events	Age (Ma)	Bioevent	DSDP Hole 547A, Magazan Plateau, Morocco (this study)	DSDP Site 137, 1000 km West of Cap Blanc, Mauritania (this study)	ODP Hole 1050C, Blake Nose (Watkins, unpublished)	ODP Hole 1052E, Blake Nose (Watkins, unpublished)	TDP Site 24, Tanzania (Ando et al., 2015)
10	96.16	FAD *Lithraphidites acutus*		284.03	510.4		
9	97.31	FAD *Cylindralithus sculptus*	623.83	350.89			41.98
8	97.93	LAD *Zeughrabdotus xenotus*			544.05		15.08
7		LAD *Eiffellithus paragogus*		287.09	554.79		60.58
6	99.94	LAD *Gartnerago chiasta*	507.53	347.71			
5	100.03	LAD *Watznaueria britannica*	600.34	347.71	527.3		25.46
4	100.45	FAD *Corollithion kennedyi*	604.8	347.71	548.95	489.08	59.66
3	100.5	FAD *Calculites anfractus*	643.51			494.08	
2		LAD *Gartnerago stenostaurion*	501.88	347.71	554.79	504.32	
1	100.84	LAD *Hayesites albiensis*	659.28	379.36	558.72	526.8	

Table 2. Bioevents and their assigned ages according to the geologic time scale (Gradstein et al., 2012). The events highlighted in grey do not occur in chronological order in the corresponding sections.

Position	Range	Event
16	0	*Lithraphidites acutus*-FAD
15	-1	*Broinsonia gammation*-LAD
14	0-1	*Calcicalathina alta*-LAD
13	0	*Staurolithites mutterlosei*-LAD
12	0	*Gartnerago segmentatum*-FAD
11	0	*Watznaueria britannica*-LAD
10	-4	*Calculites anfractus*-LAD
9	0-1	*Corollithion kennedyi*-FAD
8	0	*Lithraphidites eccentricum*-FAD
7	0	*Gartnerago stenostaurion* -LAD
6	-1	*Laguncula dorotheae*-LAD
5	-3	*Calculites anfractus*-FAD
4	0-1	*Braarudosphaera africana*-LAD
3	0	*Braarudosphaera stenorhetha*-LAD
2	0	*Hayesites albiensis*-LAD
1	0	*Braarudosphaera primula*-LAD

Table. 3. Bioevent ranking derived from unitary associations (UA) analysis; “Range” indicates the number of penalty points assigned to each bioevent.

Species	Event	Depth of bioevent	Bralower et al. (1988)	Method A Bergen et al. (2013)	Method B Bergen et al. (2013)	Probability of Success (this study)
Lithraphidites acutus	FAD	269.47				
Staurolithites mutterlosei	LAD	299.43	0.165	7	45.8	13.87 (Strong)
*Gartnerago segmentatum**	FAD	302.79		1	15.4	
*Corollithion kennedyi**	FAD	346.32		3	61.5	6.2 (Weak)
Lithraphidites eccentricum	FAD	346.32	0.165	10	96.2	14.78 (Strong)
*Laguncula dorotheae**	LAD	347.71				
Watznaueria britannica	LAD	349.12				
*Broinsonia stenostaurion**	LAD	349.12		1	18.5	
Gartnerago chiasta	LAD	349.12				
*Cylindralithus sculptus**	FAD	349.12		4	25.0	7.91 (Weak)
Hayesites albiensis	LAD	380.82				

Table 4. Calculated reliability indices for methods proposed by Bralower et al. (1988), Bergen et al. (2013) and this study for DSDP Site 137. Species whose range did not span 10 samples were excluded from this calculation and are identified as emboldened. Asterisks denote species that are absent in the sample above their FAD or below their LAD.

Species	Event	Depth of bioevent	Bralower et al. (1988)	Method A Bergen et al. (2013)	Method B Bergen et al. (2013)	Probability of Success (this study)
*Gartnerago theta**	LAD	442.86		3	18.9	6.2 (Weak)
Staurolithites mutterlosei	LAD	469.13	0.09	8	50.0	13.87 (Strong)
*Gartnerago segmentatum**	FAD	497.74		1	6.7	
Broinsonia stenostaurion	LAD	507.53	0.09	9	90.0	14.5 (Strong)
*Gartnerago chiasta**	LAD	509.27		5	63.6	10.78 (Moderate)
Corollithion kennedyi	FAD	536.64	0.09	10	100.0	14.78 (Strong)
*Laguncula dorotheae**	LAD	547.13		3	22.2	6.2 (Weak)
*Lithraphidites eccentricum**	FAD	588.62		8	59.4	13.87 (Strong)
Watznaueria britannica	LAD	604.80	0.08			
Braarudosphaera africana	LAD	623.83	0.04			
*Cylindralithus sculptus**	FAD	623.83		3	34.3	6.2 (Weak)
Calculites anfractus	LAD	632.51				
Braarudosphaera stenorhetha	LAD	659.28				
Hayesites albiensis	LAD	659.28				
Braarudosphaera primula	LAD	659.28				

Table 5. Calculated reliability indices for methods proposed by Bralower et al. (1988), Bergen et al. (2013) and this study for DSDP Site 547. Species whose range did not span 10 samples were excluded from this calculation and are identified as emboldened. Asterisks denote species that are absent in the sample above their FAD or below their LAD.

8. References

Agterberg, F. P. (1985). Normality testing and comparison of RASC to Unitary Associations Method. *In*: Gradstein, F. M., Agterberg, F. P., Brower, J. C., and Schwarzacher, W. S. (Eds.), *Quantitative stratigraphy. Kluwer, Dordrecht*, 243-278.

Agterberg, F. P. (1990). "Rank Correlation and Precision of Scaled Optimum Sequence." *Automated Stratigraphic Correlation (Vol.13)*, Elsevier New York, 239-310.

Agterberg, F. P., & Gradstein, F. M. (1999). The RASC method for ranking and scaling of biostratigraphic events. *Earth-Science Reviews*, **46**(1), 1-25.

Ando, A., Huber, B. T., MacLeod, K. G., & Watkins, D. K. (2015). Early Cenomanian "hot greenhouse" revealed by oxygen isotope record of exceptionally well-preserved foraminifera from Tanzania. *Paleoceanography*, **30**(11), 1556-1572.

Beckmann, J. P. (1972). The foraminifera and some associated microfossils of Sites 135 to 144. *In*: Hayes, D. E., Pimm, A. C., et al. (Eds.). *Initial Reports of the Deep Sea Drilling Project*, **14**: College Station, TX (Ocean Drilling Program), 389-421.

Bergen, J.A., Boesiger, T.M. & Pospichal, J.J. (2013). Low-latitude Oxfordian to Early Berriasian nannofossil biostratigraphy and its application to the subsurface of Eastern Texas. In: Hammes, U. and Gale, J. (Eds.), *Geology of the Haynesville Gas Shale in East Texas and West Louisiana, U.S.A. AAPG Memoir*, 69-102.

Bown, P. R. (2005). Early to mid-Cretaceous calcareous nannoplankton from the northwest Pacific Ocean, Leg 198, Shatsky Rise. *In:* Bralower, T. J., Premoli Silva, I., and Malone, M.J. (Eds.), *Proceedings of the Ocean Drilling Program, Scientific Results*, **198**: College Station, TX (Ocean Drilling Program), 1–82.

Brace, B. J., & D. K. Watkins. (2015). Global abundance decline in the productivity indicator Biscutum during the Cretaceous. *Journal of Nannoplankton Research*, **30**, 129-140.

Bralower, T. J., Monechi, S., & Thierstein, H. R. (1989). Calcareous nannofossil zonation of the Jurassic-Cretaceous boundary interval and correlation with the geomagnetic polarity timescale. *Marine Micropaleontology*, **14**(1), 153-235.

Bukry, D. (1972). Further comments on coccolith stratigraphy, Leg 12, Deep Sea Drilling Project. *In:* Laughton, A. S., Berggren, W. A., et al., *Initial Reports of the Deep Sea Drilling Project*, **12**: College Station, TX (Ocean Drilling Program), 1071-1084.

Burnett, J. A., L. T. Gallagher, and M. J. Hampton. (1998). "Upper cretaceous." Calcareous nannofossil biostratigraphy, British Micropaleontology Society Publication Series, 132-199.

Clarke, L. J., & Jenkyns, H. C. (1999). New oxygen isotope evidence for long-term Cretaceous climatic change in the Southern Hemisphere. *Geology*, **27**(8), 699-702.

Erbacher, J., Thurow, J., Littke, R. (1996). Evolution patterns of radiolaria and organic matter variations; a new approach to identify sea-level changes in Mid-Cretaceous pelagic environments. *Geology*, 24, 499 - 502.

Friedrich, O., Erbacher, J., Moriya, K., Wilson, P. A., & Kuhnert, H. (2008). Warm saline intermediate waters in the Cretaceous tropical Atlantic Ocean. *Nature Geoscience*, **1**(7), 453-457.

Gradstein, F. M., Ogg, G., & Schmitz, M. (2012). *The Geologic Time Scale 2012 2-Volume Set*. Elsevier Amsterdam, 1122.

Guex, J. (1991). *Biochronological correlations*. Springer-Verlag Berlin Heidelberg New York, 252.

Haq, B. U., Hardenbol, J., & Vail, P. R. (1987). Chronology of fluctuating sea levels since the Triassic. *Science*, **235**(4793), 1156-1167.

Hardas, P., & Mutterlose, J. (2006). Calcareous nannofossil biostratigraphy of the Cenomanian/Turonian boundary interval of ODP Leg 207 at the Demerara Rise. *Revue de Micropaléontologie* **49**(3), 165-179.

Hay, W.W. (1972). Probabilistic Stratigraphy. *Eclogae Geologicae Helvetiae*, **65**, 255-266.

Hay, W.W., DeConto, R.M., Wold, C.N., Wilson, K.M., Voigt, S., Schulz, M., Wold, A.R., Wolf-Christian, D., Ronov, A.B., Balukhovsky, A.N., & Soding, E. (1999). Alternative global Cretaceous paleogeography. *Evolution of the Cretaceous ocean-climate systems*. *Geological Society of America*, Boulder, Colorado: 1-47. Special Paper 332.

Hay, W. W. (2008). Evolving ideas about the Cretaceous climate and ocean circulation. *Cretaceous Research*, **29**(5), 725-753.

Hill III, M. E. (1976). Lower Cretaceous calcareous nannofossils from Texas and Oklahoma. *Palaeontographica Abteilung*, **156**(B), 103-179.

Huber, B. T., Norris, R. D., & MacLeod, K. G. (2002). Deep-sea paleotemperature record of extreme warmth during the Cretaceous. *Geology*, **30**(2), 123-126.

Jacobs, L. L., Mateus, O., Polcyn, M. J., Schulp, A. S., Scotese, C. R., Goswami, A., & Neto, A. B. (2009). Cretaceous paleogeography, paleoclimatology, and amniote biogeography of the low and mid-latitude South Atlantic Ocean. *Bulletin de la Société Géologique de France*, **180**(4), 333-341.

Jenkyns, H. C., Gale, A. S., Corfield, R. M. (1994). Carbon- and oxygen- isotope stratigraphy of the English Chalk and Italian Scaglia and its paleoclimatic significance. *Geology Magazine*, 131, 1-34.

Kennedy, W. J., Gale, A. S., Lees, J. A., & Caron, M. (2004). The global boundary stratotype section and point (GSSP) for the base of the Cenomanian Stage, Mont Risou, Hautes-Alpes, France. *Episodes-Newsmagazine of the International Union of Geological Sciences*, **27**(1), 21-32.

Leckie, R. M. (1984). Mid-Cretaceous planktonic foraminiferal biostratigraphy off Central Morocco, Deep-Sea Drilling Project Leg-79, Site-545 and Site-547. *Initial Reports of the Deep Sea Drilling Project*, **79**, 579-620.

Moriya, K., Wilson, P. A., Friedrich, O., Erbacher, J., & Kawahata, H. (2007). Testing for ice sheets during the mid-Cretaceous greenhouse using glassy foraminiferal calcite from the mid-Cenomanian tropics on Demerara Rise. *Geology*, **35**(7), 615-618.

Nederbragt, A. J., Fiorentino, A., & Klosowska, B. (2001). Quantitative analysis of calcareous microfossils across the Albian–Cenomanian boundary oceanic anoxic event at DSDP Site 547 (North Atlantic). *Palaeogeography, Palaeoclimatology, Palaeoecology*, **166**(3), 401-421.

ODSN Plate Tectonic Reconstruction Service 2011. Based on Hay, W. W. et al. (1999). Located at http://www. odsn. de/odsn/ services/paleomap/paleomap. html

Perch-Nielsen, K. (1985). Mesozoic calcareous nannofossils. *In:* H.M. Bolli, J.B. Saunders & K. Perch-Nielsen (Eds). *Plankton Stratigraphy*. Cambridge University Press, Cambridge: 329–426.

Petrizzo, M. R., Caron, M., & Silva, I. P. (2015). Remarks on the identification of the Albian/Cenomanian boundary and taxonomic clarification of the planktonic foraminifera index species Globotruncanoides, Brotzeni and Tehamaensis. *Geological Magazine*, **152**(03), 521-536.

Pletsch, T., Erbacher, J., Holbourn, A. E. L., Kuhnt, W., Moullade, M., Oboh-Ikuenobede, F. E., & Wagner, T. (2001). Cretaceous separation of Africa and South America: the view from the West African margin (ODP Leg 159). *Journal of South American Earth Sciences*, **14**(2), 147-174.

Robaszynski, F., Amédro, F., Gonzalez-Donoso, J. M.& Linares, D. (2008). The Albian (Vraconian) – Cenomanian boundary at the western Tethyan margin (Central Tunisia and southeastern France*). Bulletin de la Société géologique de France* **179**(3), 245-266.

Roth, P. H., & Thierstein, H.R. (1972). Calcareous nannoplankton: Leg 14. *In*: Hayes, D. E., Pimm, A. C., et al. (Eds.). *Initial Reports of the Deep Sea Drilling Project*, **14**: College Station, TX (Ocean Drilling Program), 389-421.

Shipboard Scientific Party, 1984. Site 547. *In:* Baumgartner, P.O., Leckie, R.M., et al., *Proceedings of the Ocean Drilling Program, Initial Reports*, **79**: College Station, TX (Ocean Drilling Program), 223-361.

Sigal, J. (1977). Essai de zonation du Crétacé méditerranéen à l'aide des foraminifères planctoniques. *Géologie Méditerranéenne* (4), 99–108.

Watkins, D.K. & Bowdler, J.L. (1984). Cretaceous calcareous nannofossils from Deep Sea Drilling Project Leg 77, southeast Gulf of Mexico. *Initial Reports of the DSDP*, **77**, 649-674.

Watkins, D. K., & Bergen, J. A. (2003). Late Albian adaptive radiation in the calcareous nannofossil genus *Eiffellithus*. *Micropaleontology*, **49**(3), 231-251.

Watkins, D. K., Cooper, M. J., & Wilson, P. A. (2005). Calcareous nannoplankton response to late Albian oceanic anoxic event 1d in the western North Atlantic. *Paleoceanography*, **20**(2).

Wiegand, G. E. (1984). Cretaceous Nannofossils from the Northwest African Margin, Deep-Sea Drilling Project Leg-79. *Initial Reports of the Deep Sea Drilling Project*, **79**, 563-578.

Wilson, P. A., Norris, R. D., & Cooper, M. J. (2002). Testing the Cretaceous greenhouse hypothesis using glassy foraminiferal calcite from the core of the Turonian tropics on Demerara Rise. *Geology*, **30**(7), 607-610.

Winterer, E. L., & Hinz, K. (1984). The Evolution of the Magazan Continental-Margin-a synthesis of geophysical and geological data with the results of drilling during Deep-Sea Drilling Project Leg 79. *Initial Reports of the Deep Sea Drilling Project*, **79**: College Station, TX (Ocean Drilling Program), 893-919.